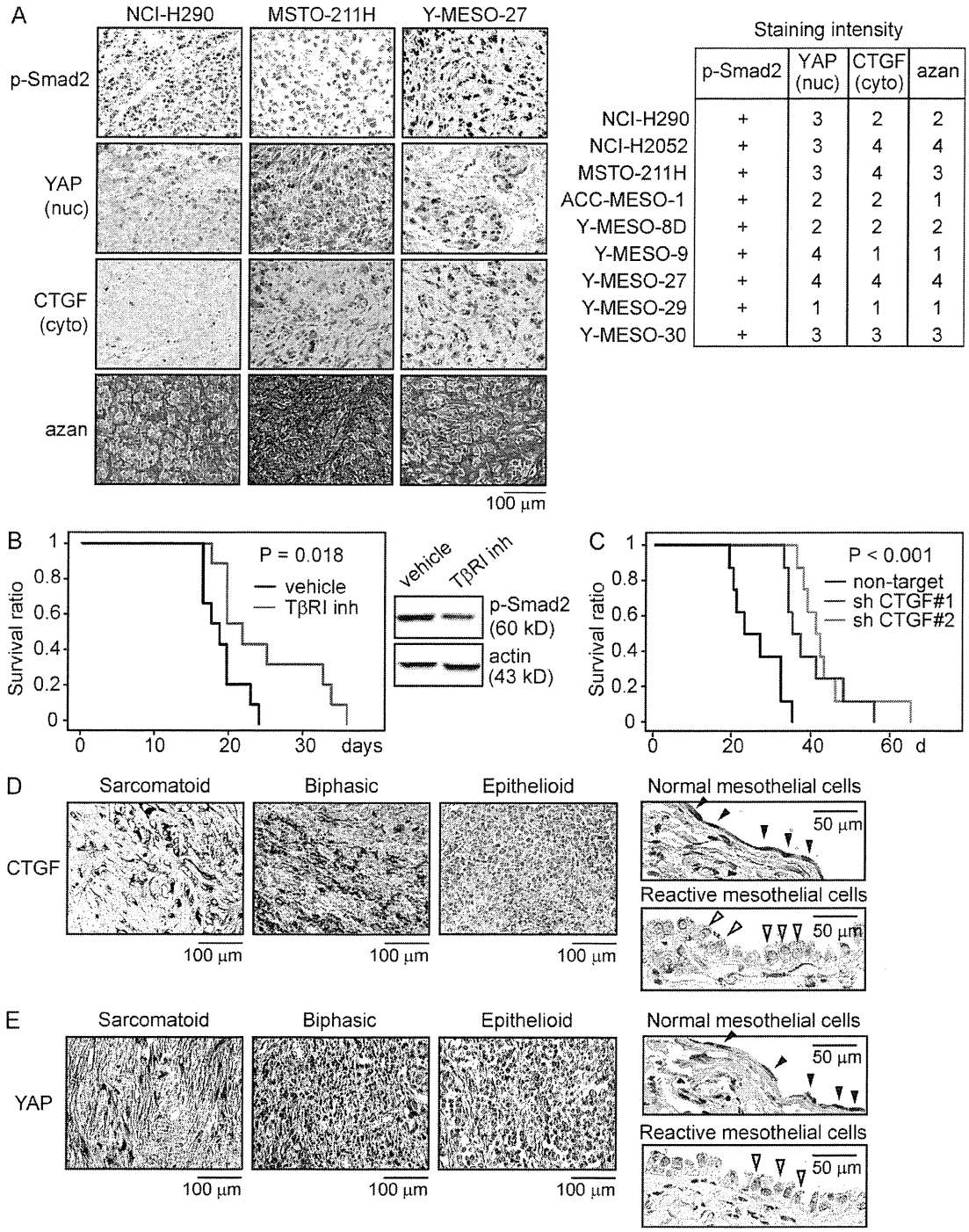

Figure 6. CTGF expression associates with the deposition of ECM protein in MM tumors. (A) Immunohistochemical staining of MM cells implanted in the thoracic cavities of athymic nude mice using p-Smad2, YAP, and CTGF antibodies. Collagen fibers were visualized in blue by azan staining (left). The right panel shows the scoring of the immunohistochemical staining. Staining intensity was scored as follows: 1, normal; 2, mild; 3, moderate; and 4, severe. (B) The Kaplan-Meier method was used to monitor the survival of athymic nude mice after the thoracic implantation of the NCI-H290 cells, followed by initiation of treatment with the TβRI inhibitor SD-208 (60 mg/kg) 2 d later (left). SD-208 was administered daily by oral gavage for 10 d (n = 9), and then tumor tissues were excised and subjected to Western blotting (right). The results shown are representative of two independent experiments. (C) NCI-H290 cells lentivirally transduced with shRNA constructs were implanted into the thoracic cavities of athymic nude mice, and survival was monitored (n = 8). The results shown are representative of three independent experiments. (D and E) Immunohistochemical staining of CTGF and YAP in MM tissues derived from patients with sarcomatoid as well as biphasic and epithelioid subtypes. Normal mesothelial cells (closed arrowheads) and reactivated normal mesothelial cells (open arrowheads) are shown in the right panels.

Table 2. CTGF expression in MM cells was dominantly observed in sarcomatoid type tissues

No.	Pathological subtype	Features	p-Smad2 (nuclear)	YAP (nuclear)	CTGF (cytoplasm)
1	Sarcomatoid	Fibrous	+	+	+
2	Sarcomatoid	Fibrous	+	+	+
3	Sarcomatoid	Fibrous	+	+	+
4	Sarcomatoid	Fibrous	+	±	+
5	Sarcomatoid	Fibrous	+	±	+
6	Sarcomatoid	Fibrous	+	+	+
7	Sarcomatoid	Fibrous	+	±	+
8	Desmoplastic (sarcomatoid)	Fibrous	+	+	+
9	Desmoplastic (sarcomatoid)	Fibrous	+	+	+
10	Biphasic	Fibrous sarcomatoid, tubulopapillary	+	S: +, E: ±	S: +, E: −
11	Biphasic	Fibrous sarcomatoid, microcystic	+	S: ±, E: ±	S: +, E: +
12	Biphasic	Fibrous sarcomatoid, solid (well-differentiated)	+	S: +, E: +	S: ±, E: ±
13	Epithelioid	Fibrous microcystic	+	+	+
14	Epithelioid	Tubulopapillary	+	−	−
15	Epithelioid	Microcystic, tubulopapillary	+	+	±
16	Epithelioid	Tubulopapillary	+	−	−
17	Epithelioid	Tubulopapillary	+	−	−
18	Epithelioid	Tubulopapillary	+	−	−
19	Epithelioid	Tubulopapillary	+	−	−
20	Epithelioid	Microcystic	+	+	−
21	Epithelioid	Tubulopapillary	+	+	−
22	Epithelioid	Tubulopapillary	+	+	±
23	Epithelioid	Solid (well-differentiated)	+	+	−
24	Epithelioid	Tubulopapillary	+	+	−

Immunohistochemical staining of 24 patients was performed using p-Smad2, YAP, and CTGF antibodies. Tissues were classified based on pathological subtypes. +, positive; ±, partially positive; −, negative; S, sarcomatoid part; E, epithelioid part.

Expression of CTGF was controlled by the presence of the YAP–TEAD4–Smad3–p300 complex in the nucleus of the MM, which we identify as a novel therapeutic target in MM.

Consistent with previous data showing that inactivation of the *NF2* and Hippo pathway is the most frequent defect in mesothelioma, immunohistochemical analysis of MM specimens revealed overexpression and nuclear accumulation of YAP, whereas no signals were observed in normal pleural mesothelial cells (Yokoyama et al., 2008). Nuclear accumulation of YAP is responsible for MM cells undergoing oncogenic events, and normal mesothelial cells might have less YAP-dependent growth because of down-regulation by the intact Hippo pathway.

In looking for synergy between the inactivation of the Hippo pathway and TGF-β signaling, we found that knocking down YAP, which predominantly resides in the nucleus of NCI-H290 cells, affected only a small portion of TGF-β–responsive genes, suggesting that functional association between YAP and Smad2/3 only occurs under a specific situation. *CTGF* is a gene carrying both a TEAD-binding site and a consensus Smad-binding site adjacent to each other on its promoter. Although the binding between YAP and Smad3 is not overly strong, it results in an obvious synergistic activation in the reporter assay or CTGF protein expression assay. Even in the immunoprecipitation assay using HEK293 cells, the exogenous overexpression of Smad3 showed weak binding between YAP and Smad3, and we could not detect endogenous binding in mesothelioma cells. This suggests that other components may be responsible for strengthening the YAP–Smad3 binding and promoting transactivation. We found that p300 and TEAD4 are components of the Smad complex, and Smad3 preferentially binds to TEAD4 rather than to YAP. This hypothesis enabled us to determine not only the physical interactions but also the functional meanings of Smad3–TEAD4 and Smad3–YAP bindings at the endogenous level.

CTGF is a 36/38-kD cysteine-rich protein whose expression is often observed in stroma, which might reflect an active tumor–stromal interaction (Wahab and Mason, 2006). Enhancement of tumor–stromal interactions can potentially promote cancer cell invasion and metastasis. In addition to recent studies that indicate that tumor cell–derived CTGF plays an important role in the proliferation of breast cancer cells (Zhao et al., 2008) and growth of pancreatic tumors (Bennewith et al., 2009), CTGF also affects vascularization, migration, and epithelial-mesenchymal transition in the context of oncogenic properties (Wahab and Mason, 2006). Our immunohistochemical staining of MM cells implanted in the thoracic cavities of nude mice revealed that p-Smad2 constantly resided in the nucleus, whereas the level of YAP in

the nucleus varied among cells. CTGF expression was moderately correlated to YAP localization in the nucleus, consistent with our result that maximum CTGF expression was achieved by activation of TGF-β signaling and inactivation of the *NF2* tumor suppressor pathway. The high levels of YAP nuclear staining and low levels of CTGF staining seen in Y-MESO-9 cells and in some epithelioid type human MM tissues were the exception to this relationship, suggesting that there might be additional undiscovered mechanisms participating in the regulation and of CTGF expression.

Importantly, there was a strong association between MM CTGF expression and the amount of stroma surrounding MM cells. As noted in Y-MESO-29 cells, the cells that grew in solid/nodular form with thin connective tissues surrounding the mass of tumor cells tended to express rather low levels of CTGF. In contrast, NCI-H2052 and Y-MESO-27 cells, which have high levels of CTGF staining, showed extensive accumulation of collagen fibers. Approximately 60% of MM tumors show histologically epithelioid subtype, whereas sarcomatoid and biphasic types each account for 20% (Flores et al., 2007). From our findings which showed that sarcomatoid type MM tumors exhibit strong CTGF staining, we speculate that tumor-derived CTGF has a strong correlation with the deposition of surrounding connective tissue in MM tumors, further linking CTGF to MM malignancy. Our data suggest that TGF-β signaling is active in both the normal and transformed mesothelium. However, in the transformed mesothelium, the activation of the Hippo pathway synergizes with the TGF-β pathway signaling to increase CTGF production and thereby amplify the profibrotic and colony-stimulating effects of TGF-β and potentially inducing other protumorigenic effects in the microenvironment.

Determining the proper way to target CTGF expression is critical for clinical applications. To directly target CTGF, one must first decide whether to use antibody or antisense therapies. Our data also suggest that there might be additional undiscovered mechanisms that participate in the regulation of CTGF expression. Furthermore, the mechanism that allows CTGF to exert its effects has not yet been clarified. Further research regarding CTGF expression and its functions might lead to the discovery of new targets that could be used to regulate CTGF expression. The number of available targets could be increased if TGF-β and Hippo signaling pathways were included. There are some studies indicating that systemic administration of TGF-β antagonists can suppress the growth of mesotheliomas primarily through the reactivation of antitumor immune responses (Suzuki et al., 2004, 2007). In this study, we demonstrated that these antagonists have an important mechanistic contribution to the tumor parenchyma as well. The TGF-β type I receptor inhibitor or TGF-β antibody might be suitable for suppressing the activation of the TGF-β pathway and further attenuate CTGF expression in MM. Regarding the Hippo signaling pathway, drugs that inhibit YAP translocation into the nucleus or activate Hippo signaling are expected to be developed. Simultaneous suppression of both the TGF-β and Hippo signaling pathways may considerably reduce CTGF expression. Our findings propose Smad3 and YAP to be the factors influencing expression of CTGF, and we show for the first time that CTGF might be a strong candidate for molecularly targeted therapy, affecting both mesothelioma cell growth and the tumor microenvironment.

MATERIALS AND METHODS

Cell culture and reagents. HEK293 cells were grown in Dulbecco's Modified Eagle's Medium (Invitrogen) supplemented with 10% FBS. MeT-5A, NCI-H2052, and MSTO-211H cells were purchased from the American Type Culture Collection. NCI-H290 cells were gifts from A.F. Gazdar (University of Texas Southwestern Medical Center, Dallas, TX). ACC-MESO-1, Y-MESO-8D, 9, 14, 27, 29, and 30 cells were established in our laboratory, as reported previously (Taniguchi et al., 2007). All MM cell lines were cultured in RPMI 1640 (Invitrogen) supplemented with 10% FBS. Human recombinant TGF-β1 was purchased from R&D Systems. SD-208 (2,4-disubstituted pteridine; an ATP-competitive inhibitor of TGF-β RI kinase) was purchased from Sigma-Aldrich or synthesized by Epichem Pty Ltd. and dissolved in DMSO as 10-μM stocks or at 7.5 mg/ml with 0.5% (wt/vol) methylcellulose.

Soft agar colony formation assay. The soft agar colony formation assay was performed using standard techniques. MeT-5A cells were trypsinized, and 2×10^4 cells were plated in 0.3% top agarose and cultured for 7 d.

Western blot and immunoprecipitation analysis. Cells were washed with ice-cold PBS, lysed on ice for 30 min in lysis buffer (10 mM Hepes, 200 mM NaCl, 30 mM sodium pyrophosphate, 50 mM NaF, 5 μM $ZnCl_2$, and 1.0% Triton X-100, pH 7.5) supplemented with protease inhibitor cocktail (Roche), and centrifuged at 12,000 *g* for 20 min. Supernatants were immunoprecipitated with Immunoprecipitation kit–Dynabeads Protein G (Invitrogen) according to the manufacturer's instructions, using anti-YAP (63.7; Santa Cruz Biotechnology, Inc.), p300 (C-20; Santa Cruz Biotechnology, Inc.), TEAD4 (aa 151–260; Abnova), Smad2/3 (BD and Cell Signaling Technology), HA (Y-11; Santa Cruz Biotechnology, Inc.), or FLAG (M2; Sigma-Aldrich) antibody. Immunoprecipitated proteins were resolved by 10% Tris-glycine SDS-PAGE (Invitrogen), transferred to Immobilon-P membranes (Millipore), and detected with the appropriate primary antibody. Western blots were prepared by standard procedures using anti–p-Smad2/3 (Cell Signaling Technology), YAP1 (EP1674Y; Abcam), CTGF (L-20; Santa Cruz Biotechnology, Inc.), actin monoclonal (Millipore), and other antibodies described above. Immunoreactivity was detected by ECL (GE Healthcare).

Transcriptional reporter assays. Luciferase assays were performed using the Dual-Luciferase Reporter Assay System (Promega) in which Renilla luciferase plasmids were cotransfected as a control to standardize the transfection efficiency. All activity results are normalized to Renilla expression and are representative of three independent assays.

RNA interference vectors in human MM cells. To generate lentivirus that transcribes shRNA, short hairpin oligonucleotides were inserted into pLentiLox 3.7 containing the U6 promoter and PLKO.1 (Sigma-Aldrich) and transfected into HEK293FT cells together with VSVG, RSV-REV, and pMDLg/pRRE. Short hairpin oligonucleotides for YAP (Yokoyama et al., 2008) and CTGF (Zhao et al., 2008) were designed as described previously. A plasmid vector containing the U6 promoter and puromycin-resistance gene was used for transient expression of shYAP (Yokoyama et al., 2008).

Expression profiling with microarrays. Extracted mRNA was subjected to generate cRNA, which was labeled with Cy3 or Cy5 (GE Healthcare) using a low RNA Fluorescent Linear Amplification kit (Agilent Technologies) according to the manufacturer's protocol. Labeled cRNA was then hybridized to an Agilent 44K Whole Human Genome Microarray, followed by confocal laser scanning (Agilent Technologies). The microarray data have been deposited in ArrayExpress under accession no. E-TABM-1144.

Real-time RT-PCR. Quantitative real-time RT-PCR was performed using first-strand complementary DNA with the TaqMan Universal PCR Master Mix (Applied Biosystems), and amplification was performed with an ABI 7500 Real-time PCR System (Applied Biosystems) according to the manufacturer's instructions. Quantification of GAPDH transcripts as an internal control for the amount and quality of cDNA was performed for all samples.

ChIP. The ChIP assay was performed using the ChIP-IT Express Magnetic Chromatin Immunoprecipitation kit (Active Motif) according to the manufacturer's instructions, followed by real-time RT-PCR with the forward primer 5′-ATATGAATCAGGAGTGGTGCGA-3′ and reverse primer 5′-CAACTCACACCGGATTGATCC-3′. The antibodies used were anti-YAP (H-125; Santa Cruz Biotechnology, Inc.), p300 (C-20; Santa Cruz Biotechnology, Inc.), and Smad2/3 (BD). Re-ChIP-IT Magnetic Chromatin Re-Immunoprecipitation kit (Active Motif) was used for the ChIP-reChIP experiment.

Animal experiments. 7–8-wk-old female athymic nude mice of KSN strain (Shizuoka Laboratory Animal Center) were weighed and randomly assigned to different treatment groups. Lentivirally infected or uninfected NCI-H290 cells were then orthotopically injected into the right thoracic cavity of each mouse. To examine the effect of TGF-β type I receptor kinase inhibition, mice (n = 8) were daily treated with single 0.2-ml doses of 0.5% (wt/vol) methylcellulose as a vehicle or 60 mg/kg SD-208 by oral gavage as described previously (Uhl et al., 2004) for 10 d, starting 2 d after tumor cell inoculation. The experimental design was approved by the Animal Care Committee of the Aichi Cancer Center Research Institute, and the animals were cared for in accordance with institutional guidelines as well as the Guidelines for Proper Conduct of Animal Experiments (Science Council of Japan, June 1, 2006).

Immunohistochemistry. The tumor-bearing mice were sacrificed under deep anesthesia and excised the intrathoracic tumor tissue, which was fixed in 10% neutral-buffered formalin and processed for histopathological (hematoxylin and eosin and azan staining) and immunohistochemical examination using an indirect immunoperoxidase method. The antibodies used for immunohistochemical staining were anti–p-Smad2, p-specific (Ser 463/467; Millipore), YAP (H-125; Santa Cruz Biotechnology, Inc.), and CTGF (L-20; Santa Cruz Biotechnology, Inc.).

Statistical analysis. Survival period was analyzed by the Kaplan-Meier method and compared using the log-rank test. All reported p-values were two-sided, with $P < 0.05$ considered statistically significant. Calculations were performed with StatView software version 5.0 (Abacus Concepts).

Online supplemental material. Fig. S1 shows that TGF-β affects the signaling of MM cells. Online supplemental material is available at http://www.jem.org/cgi/content/full/jem.20111653/DC1.

We thank L.M. Wakefield and A. Hata for comments on the manuscript and K.C. Flanders, K. Kawaguchi, T. Mizuno, F. Ishiguro, K. Shinjo, and T. Matsuki for useful discussions. We thank M. Kizuki, N. Saito, and M. Tsuji for excellent technical assistance.

This work was supported by funds from the 24th General Assembly of the Japanese Association of Medical Sciences (to M. Fujii), funds from the Aichi Cancer Research Foundation (to M. Fujii), and Grants-in-Aid for Scientific Research from the Japan Society for the Promotion of Science (20590420 and 23592788 to M. Fujii) and partly by a Special Coordination Fund for Promoting Science and Technology from the Ministry of Education, Culture, Sports, Science and Technology of Japan (H18-1-3-3-1 to Y. Sekido), Grants-in-Aid for Scientific Research (22300338 to Y. Sekido), Grants-in-aid for Third-Term Comprehensive Control Research for Cancer from the Ministry of Health, Labor and Welfare of Japan (to Y. Sekido), the Takeda Science Foundation (Y. Sekido), and the Kobayashi Foundation for Cancer Research (Y. Sekido).

The authors have no additional financial interests.

Submitted: 8 August 2011
Accepted: 12 January 2012

REFERENCES

Alarcón, C., A.I. Zaromytidou, Q. Xi, S. Gao, J. Yu, S. Fujisawa, A. Barlas, A.N. Miller, K. Manova-Todorova, M.J. Macias, et al. 2009. Nuclear CDKs drive Smad transcriptional activation and turnover in BMP and TGF-β pathways. *Cell.* 139:757–769. http://dx.doi.org/10.1016/j.cell.2009.09.035

Anzano, M.A., A.B. Roberts, J.M. Smith, M.B. Sporn, and J.E. De Larco. 1983. Sarcoma growth factor from conditioned medium of virally transformed cells is composed of both type α and type β transforming growth factors. *Proc. Natl. Acad. Sci. USA.* 80:6264–6268. http://dx.doi.org/10.1073/pnas.80.20.6264

Bennewith, K.L., X. Huang, C.M. Ham, E.E. Graves, J.T. Erler, N. Kambham, J. Feazell, G.P. Yang, A. Koong, and A.J. Giaccia. 2009. The role of tumor cell-derived connective tissue growth factor (CTGF/CCN2) in pancreatic tumor growth. *Cancer Res.* 69:775–784. http://dx.doi.org/10.1158/0008-5472.CAN-08-0987

Bianchi, A.B., S.I. Mitsunaga, J.Q. Cheng, W.M. Klein, S.C. Jhanwar, B. Seizinger, N. Kley, A.J. Klein-Szanto, and J.R. Testa. 1995. High frequency of inactivating mutations in the neurofibromatosis type 2 gene (NF2) in primary malignant mesotheliomas. *Proc. Natl. Acad. Sci. USA.* 92:10854–10858. http://dx.doi.org/10.1073/pnas.92.24.10854

de Larco, J.E., and G.J. Todaro. 1978. Growth factors from murine sarcoma virus-transformed cells. *Proc. Natl. Acad. Sci. USA.* 75:4001–4005. http://dx.doi.org/10.1073/pnas.75.8.4001

Dong, J., G. Feldmann, J. Huang, S. Wu, N. Zhang, S.A. Comerford, M.F. Gayyed, R.A. Anders, A. Maitra, and D. Pan. 2007. Elucidation of a universal size-control mechanism in *Drosophila* and mammals. *Cell.* 130:1120–1133. http://dx.doi.org/10.1016/j.cell.2007.07.019

Dunn, L.K., K.S. Mohammad, P.G. Fournier, C.R. McKenna, H.W. Davis, M. Niewolna, X.H. Peng, J.M. Chirgwin, and T.A. Guise. 2009. Hypoxia and TGF-β drive breast cancer bone metastases through parallel signaling pathways in tumor cells and the bone microenvironment. *PLoS ONE.* 4:e6896. http://dx.doi.org/10.1371/journal.pone.0006896

Flores, R.M., M. Zakowski, E. Venkatraman, L. Krug, K. Rosenzweig, J. Dycoco, C. Lee, C. Yeoh, M. Bains, and V. Rusch. 2007. Prognostic factors in the treatment of malignant pleural mesothelioma at a large tertiary referral center. *J. Thorac. Oncol.* 2:957–965. http://dx.doi.org/10.1097/JTO.0b013e31815608d9

Fujii, M., L.A. Lyakh, C.P. Bracken, J. Fukuoka, M. Hayakawa, T. Tsukiyama, S.J. Soll, M. Harris, S. Rocha, K.C. Roche, et al. 2006. SNIP1 is a candidate modifier of the transcriptional activity of c-Myc on E box-dependent target genes. *Mol. Cell.* 24:771–783. http://dx.doi.org/10.1016/j.molcel.2006.11.006

Gabrielson, E.W., B.I. Gerwin, C.C. Harris, A.B. Roberts, M.B. Sporn, and J.F. Lechner. 1988. Stimulation of DNA synthesis in cultured primary human mesothelial cells by specific growth factors. *FASEB J.* 2:2717–2721.

Gerwin, B.I., J.F. Lechner, R.R. Reddel, A.B. Roberts, K.C. Robbins, E.W. Gabrielson, and C.C. Harris. 1987. Comparison of production of transforming growth factor-β and platelet-derived growth factor by normal human mesothelial cells and mesothelioma cell lines. *Cancer Res.* 47:6180–6184.

Hamaratoglu, F., M. Willecke, M. Kango-Singh, R. Nolo, E. Hyun, C. Tao, H. Jafar-Nejad, and G. Halder. 2006. The tumour-suppressor genes NF2/Merlin and Expanded act through Hippo signalling to regulate cell proliferation and apoptosis. *Nat. Cell Biol.* 8:27–36. http://dx.doi.org/10.1038/ncb1339

Hay, B.A., and M. Guo. 2003. Coupling cell growth, proliferation, and death. Hippo weighs in. *Dev. Cell.* 5:361–363. http://dx.doi.org/10.1016/S1534-5807(03)00270-3

Holmes, A., D.J. Abraham, S. Sa, X. Shiwen, C.M. Black, and A. Leask. 2001. CTGF and SMADs, maintenance of scleroderma phenotype is independent of SMAD signaling. *J. Biol. Chem.* 276:10594–10601. http://dx.doi.org/10.1074/jbc.M010149200

Ke, Y., R.R. Reddel, B.I. Gerwin, H.K. Reddel, A.N. Somers, M.G. McMenamin, M.A. LaVeck, R.A. Stahel, J.F. Lechner, and C.C. Harris. 1989. Establishment of a human in vitro mesothelial cell model system for investigating mechanisms of asbestos-induced mesothelioma. *Am. J. Pathol.* 134:979–991.

Levental, K.R., H. Yu, L. Kass, J.N. Lakins, M. Egeblad, J.T. Erler, S.F. Fong, K. Csiszar, A. Giaccia, W. Weninger, et al. 2009. Matrix crosslinking forces tumor progression by enhancing integrin signaling. *Cell.* 139:891–906. http://dx.doi.org/10.1016/j.cell.2009.10.027

Massagué, J. 2008. TGFbeta in cancer. *Cell.* 134:215–230. http://dx.doi.org/10.1016/j.cell.2008.07.001

Massagué, J., J. Seoane, and D. Wotton. 2005. Smad transcription factors. *Genes Dev.* 19:2783–2810. http://dx.doi.org/10.1101/gad.1350705

Moses, H.L., E.L. Branum, J.A. Proper, and R.A. Robinson. 1981. Transforming growth factor production by chemically transformed cells. *Cancer Res.* 41:2842–2848.

Murakami, H., T. Mizuno, T. Taniguchi, M. Fujii, F. Ishiguro, T. Fukui, S. Akatsuka, Y. Horio, T. Hida, Y. Kondo, et al. 2011. LATS2 is a tumor suppressor gene of malignant mesothelioma. *Cancer Res.* 71:873–883. http://dx.doi.org/10.1158/0008-5472.CAN-10-2164

Murayama, T., K. Takahashi, Y. Natori, and N. Kurumatani. 2006. Estimation of future mortality from pleural malignant mesothelioma in Japan based on an age-cohort model. *Am. J. Ind. Med.* 49:1–7. http://dx.doi.org/10.1002/ajim.20246

Nishihara, A., J.I. Hanai, N. Okamoto, J. Yanagisawa, S. Kato, K. Miyazono, and M. Kawabata. 1998. Role of p300, a transcriptional coactivator, in signalling of TGF-β. *Genes Cells.* 3:613–623. http://dx.doi.org/10.1046/j.1365-2443.1998.00217.x

Radisky, E.S., and D.C. Radisky. 2007. Stromal induction of breast cancer: inflammation and invasion. *Rev. Endocr. Metab. Disord.* 8:279–287. http://dx.doi.org/10.1007/s11154-007-9037-1

Roberts, A.B., and L.M. Wakefield. 2003. The two faces of transforming growth factor β in carcinogenesis. *Proc. Natl. Acad. Sci. USA.* 100:8621–8623. http://dx.doi.org/10.1073/pnas.1633291100

Roberts, A.B., F. Tian, S.D. Byfield, C. Stuelten, A. Ooshima, S. Saika, and K.C. Flanders. 2006. Smad3 is key to TGF-β-mediated epithelial-to-mesenchymal transition, fibrosis, tumor suppression and metastasis. *Cytokine Growth Factor Rev.* 17:19–27. http://dx.doi.org/10.1016/j.cytogfr.2005.09.008

Robinson, B.W., and R.A. Lake. 2005. Advances in malignant mesothelioma. *N. Engl. J. Med.* 353:1591–1603. http://dx.doi.org/10.1056/NEJMra050152

Ryoo, H.D., and H. Steller. 2003. Hippo and its mission for growth control. *Nat. Cell Biol.* 5:853–855. http://dx.doi.org/10.1038/ncb1003-853

Sekido, Y. 2010. Genomic abnormalities and signal transduction dysregulation in malignant mesothelioma cells. *Cancer Sci.* 101:1–6. http://dx.doi.org/10.1111/j.1349-7006.2009.01336.x

Sekido, Y., H.I. Pass, S. Bader, D.J. Mew, M.F. Christman, A.F. Gazdar, and J.D. Minna. 1995. Neurofibromatosis type 2 (NF2) gene is somatically mutated in mesothelioma but not in lung cancer. *Cancer Res.* 55:1227–1231.

Suzuki, E., V. Kapoor, H.K. Cheung, L.E. Ling, P.A. DeLong, L.R. Kaiser, and S.M. Albelda. 2004. Soluble type II transforming growth factor-β receptor inhibits established murine malignant mesothelioma tumor growth by augmenting host antitumor immunity. *Clin. Cancer Res.* 10:5907–5918. http://dx.doi.org/10.1158/1078-0432.CCR-03-0611

Suzuki, E., S. Kim, H.K. Cheung, M.J. Corbley, X. Zhang, L. Sun, F. Shan, J. Singh, W.C. Lee, S.M. Albelda, and L.E. Ling. 2007. A novel small-molecule inhibitor of transforming growth factor β type I receptor kinase (SM16) inhibits murine mesothelioma tumor growth in vivo and prevents tumor recurrence after surgical resection. *Cancer Res.* 67:2351–2359. http://dx.doi.org/10.1158/0008-5472.CAN-06-2389

Taniguchi, T., S. Karnan, T. Fukui, T. Yokoyama, H. Tagawa, K. Yokoi, Y. Ueda, T. Mitsudomi, Y. Horio, T. Hida, et al. 2007. Genomic profiling of malignant pleural mesothelioma with array-based comparative genomic hybridization shows frequent non-random chromosomal alteration regions including JUN amplification on 1p32. *Cancer Sci.* 98:438–446. http://dx.doi.org/10.1111/j.1349-7006.2006.00386.x

Tsao, A.S., I. Wistuba, J.A. Roth, and H.L. Kindler. 2009. Malignant pleural mesothelioma. *J. Clin. Oncol.* 27:2081–2090. http://dx.doi.org/10.1200/JCO.2008.19.8523

Uhl, M., S. Aulwurm, J. Wischhusen, M. Weiler, J.Y. Ma, R. Almirez, R. Mangadu, Y.W. Liu, M. Platten, U. Herrlinger, et al. 2004. SD-208, a novel transforming growth factor β receptor I kinase inhibitor, inhibits growth and invasiveness and enhances immunogenicity of murine and human glioma cells in vitro and in vivo. *Cancer Res.* 64:7954–7961. http://dx.doi.org/10.1158/0008-5472.CAN-04-1013

Varelas, X., R. Sakuma, P. Samavarchi-Tehrani, R. Peerani, B.M. Rao, J. Dembowy, M.B. Yaffe, P.W. Zandstra, and J.L. Wrana. 2008. TAZ controls Smad nucleocytoplasmic shuttling and regulates human embryonic stem-cell self-renewal. *Nat. Cell Biol.* 10:837–848. http://dx.doi.org/10.1038/ncb1748

Varelas, X., P. Samavarchi-Tehrani, M. Narimatsu, A. Weiss, K. Cockburn, B.G. Larsen, J. Rossant, and J.L. Wrana. 2010. The Crumbs complex couples cell density sensing to Hippo-dependent control of the TGF-β-SMAD pathway. *Dev. Cell.* 19:831–844. http://dx.doi.org/10.1016/j.devcel.2010.11.012

Vassilev, A., K.J. Kaneko, H. Shu, Y. Zhao, and M.L. DePamphilis. 2001. TEAD/TEF transcription factors utilize the activation domain of YAP65, a Src/Yes-associated protein localized in the cytoplasm. *Genes Dev.* 15:1229–1241. http://dx.doi.org/10.1101/gad.888601

Wahab, N.A., and R.M. Mason. 2006. A critical look at growth factors and epithelial-to-mesenchymal transition in the adult kidney. Interrelationships between growth factors that regulate EMT in the adult kidney. *Nephron, Exp. Nephrol.* 104:e129–e134. http://dx.doi.org/10.1159/000094963

Wang, K., C. Degerny, M. Xu, and X.J. Yang. 2009. YAP, TAZ, and Yorkie: a conserved family of signal-responsive transcriptional coregulators in animal development and human disease. *Biochem. Cell Biol.* 87:77–91. http://dx.doi.org/10.1139/O08-114

Wu, S., J. Huang, J. Dong, and D. Pan. 2003. hippo encodes a Ste-20 family protein kinase that restricts cell proliferation and promotes apoptosis in conjunction with salvador and warts. *Cell.* 114:445–456. http://dx.doi.org/10.1016/S0092-8674(03)00549-X

Xiao, L., L. Sun, F.Y. Liu, Y.M. Peng, and S.B. Duan. 2010. Connective tissue growth factor knockdown attenuated matrix protein production and vascular endothelial growth factor expression induced by transforming growth factor-β1 in cultured human peritoneal mesothelial cells. *Ther. Apher. Dial.* 14:27–34. http://dx.doi.org/10.1111/j.1744-9987.2009.00701.x

Yang, Y.C., E. Piek, J. Zavadil, D. Liang, D. Xie, J. Heyer, P. Pavlidis, R. Kucherlapati, A.B. Roberts, and E.P. Böttinger. 2003. Hierarchical model of gene regulation by transforming growth factor β. *Proc. Natl. Acad. Sci. USA.* 100:10269–10274. http://dx.doi.org/10.1073/pnas.1834070100

Yokoyama, T., H. Osada, H. Murakami, Y. Tatematsu, T. Taniguchi, Y. Kondo, Y. Yatabe, Y. Hasegawa, K. Shimokata, Y. Horio, et al. 2008. YAP1 is involved in mesothelioma development and negatively regulated by Merlin through phosphorylation. *Carcinogenesis.* 29:2139–2146. http://dx.doi.org/10.1093/carcin/bgn200

Zhang, N., H. Bai, K.K. David, J. Dong, Y. Zheng, J. Cai, M. Giovannini, P. Liu, R.A. Anders, and D. Pan. 2010. The Merlin/NF2 tumor suppressor functions through the YAP oncoprotein to regulate tissue homeostasis in mammals. *Dev. Cell.* 19:27–38. http://dx.doi.org/10.1016/j.devcel.2010.06.015

Zhao, B., X. Ye, J. Yu, L. Li, W. Li, S. Li, J. Yu, J.D. Lin, C.Y. Wang, A.M. Chinnaiyan, et al. 2008. TEAD mediates YAP-dependent gene induction and growth control. *Genes Dev.* 22:1962–1971. http://dx.doi.org/10.1101/gad.1664408

Zhao, B., J. Kim, X. Ye, Z.C. Lai, and K.L. Guan. 2009. Both TEAD-binding and WW domains are required for the growth stimulation and oncogenic transformation activity of yes-associated protein. *Cancer Res.* 69:1089–1098. http://dx.doi.org/10.1158/0008-5472.CAN-08-2997

Oncogene (2012) **31,** 5117 - 5122

www.nature.com/onc

SHORT COMMUNICATION

YAP induces malignant mesothelioma cell proliferation by upregulating transcription of cell cycle-promoting genes

T Mizuno[1,2], H Murakami[1], M Fujii[1], F Ishiguro[1,2], I Tanaka[1], Y Kondo[1], S Akatsuka[3], S Toyokuni[3], K Yokoi[2], H Osada[1,4] and Y Sekido[1,4]

Malignant mesothelioma (MM) shows frequent inactivation of the *neurofibromatosis type 2* (*NF2*) -tumor-suppressor gene. Recent studies have documented that the Hippo signaling pathway, a downstream cascade of Merlin (a product of *NF2*), has a key role in organ size control and carcinogenesis by regulating cell proliferation and apoptosis. We previously reported that MMs show overexpression of *Yes-associated protein* (YAP) transcriptional coactivator, the main downstream effector of the Hippo signaling pathway, which results from the inactivation of *NF2*, *LATS2* and/or *SAV1 genes* (the latter two encoding core components of the mammalian Hippo pathway) or amplification of *YAP* itself. However, the detailed roles of YAP remain unclear, especially the target genes of YAP that enhance MM cell growth and survival. Here, we demonstrated that YAP-knockdown inhibited cell motility, invasion and anchorage-independent growth as well as cell proliferation of MM cells *in vitro*. We analyzed genes commonly regulated by YAP in three MM cell lines with constitutive YAP-activation, and found that the major subsets of YAP-upregulating genes encode cell cycle regulators. Among them, YAP directly induced the transcription of *CCND1* and *FOXM1*, in cooperation with TEAD transcription factor. We also found that knockdown of *CCND1* and *FOXM1* suppressed MM cell proliferation, although the inhibitory effects were less evident than those of YAP knockdown. These results indicate that constitutive YAP activation in MM cells promotes cell cycle progression giving more aggressive phenotypes to MM cells.

Oncogene (2012) **31,** 5117-5122; doi:10.1038/onc.2012.5; published online 30 January 2012

Keywords: malignant mesothelioma; Hippo pathway; YAP; CCND1; cell cycle

INTRODUCTION

Malignant mesothelioma (MM) is one of the most aggressive neoplasms, which is caused by asbestos exposure.[1,2] It is usually resistant to conventional therapies, and the prognosis of patients is very poor. The median survival of malignant pleural mesothelioma patients after diagnosis is 7-11 months.[1,3,4] There is a 30-40 year interval before clinical presentation of the tumor after asbestos exposure.[5] While the long latency of the disease implies that multiple genetic and epigenetic alterations might be required for MM progression,[6] the detailed molecular pathogenesis of MM has not been well understood.

Among the limited number of genes that are frequently mutated in MMs, inactivation of $p16^{INK4a}/p14^{ARF}$ is detected in over 70% of MMs.[7] The *NF2* gene, which is responsible for the *NF2* familial cancer syndrome, has been shown to be inactivated in 40-50% of MMs.[8,9] A recent study has also indicated that 23% of MM cases had an inactivating mutation of *BAP1*, which encodes a nuclear deubiquitinase.[10,11]

The *NF2* gene encodes Merlin, which is a membrane-cytoskeleton-associated protein with four-point-one, ezrin, radixin and moesin domain, and acts as a tumor suppressor.[12] One of the downstream signaling cascades regulated by Merlin is the Hippo signaling pathway, which is conserved from *Drosophila* to mammalians.[13-15] In MM cells, besides the *NF2* mutation, genetic alterations in the components of the Hippo signaling pathway have also been identified recently, including inactivating mutations of *large tumor suppressor 1* (*LATS1*), *LATS2* and *SAV1*, and amplification of *Yes-associated protein* (*YAP*).[10,16,17] Together with *NF2* mutation, MM shows frequent Merlin-Hippo pathway inactivation, which leads to YAP activation in over 70% of MM cases.[18]

Studies have shown that the Hippo signaling pathway is involved in the cell cycle regulation and the control of organ size.[19,20] The dysregulation of this pathway, which leads to constitutive YAP activation, induces the oncogenic transformation in cooperation with distinct transcription factors such as TEAD family members.[21-24] Overexpression, especially dominant expression in the nuclei compared with the cytoplasm of tumor cells and the oncogenic roles of YAP have been shown in various types of human malignancies.[25-29] On the other hand, the anti-proliferative or apoptosis-inducing function of YAP has also been demonstrated in the context of DNA damage or cellular stress, which induces its binding of YAP with other transcription factors such as p73, a paralog of p53 tumor suppressor.[30-32]

We previously showed that YAP promoted cell proliferation[17] and exogenous LATS2 inhibited cell proliferation via induction of YAP phosphorylation in MM cells.[16] However, the detailed characteristics of YAP oncogenic properties remain unclear, including the exact target genes that are inducible by YAP activation in MM cells. In this study, we aimed to identify the target genes of YAP in MM cells to elaborate how YAP induces the MM-cell malignant phenotypes. We found that cell cycle-regulating genes, including *CCDN1* and *FOXM1*, are induced by YAP, suggesting that the dysregulation of cell cycle regulation is one of the key alterations in which MM cells acquire malignancy by YAP activation.

[1]Division of Molecular Oncology, Aichi Cancer Center Research Institute, Nagoya, Japan; [2]Department of Thoracic Surgery, Nagoya University Graduate School of Medicine, Nagoya, Japan; [3]Department of Pathology and Biological Responses, Nagoya University Graduate School of Medicine, Nagoya, Japan and [4]Department of Cancer Genetics, Program in Function Construction Medicine, Nagoya University Graduate School of Medicine, Nagoya, Japan. Correspondence: Dr Y Sekido, Division of Molecular Oncology, Aichi Cancer Center Research Institute, Kanokoden 1-1, Chikusa-ku, Nagoya, Aichi 464-8681, Japan. E-mail: ysekido@aichi-cc.jp
Received 3 September 2011; revised 19 December 2011; accepted 30 December 2011; published online 30 January 2012

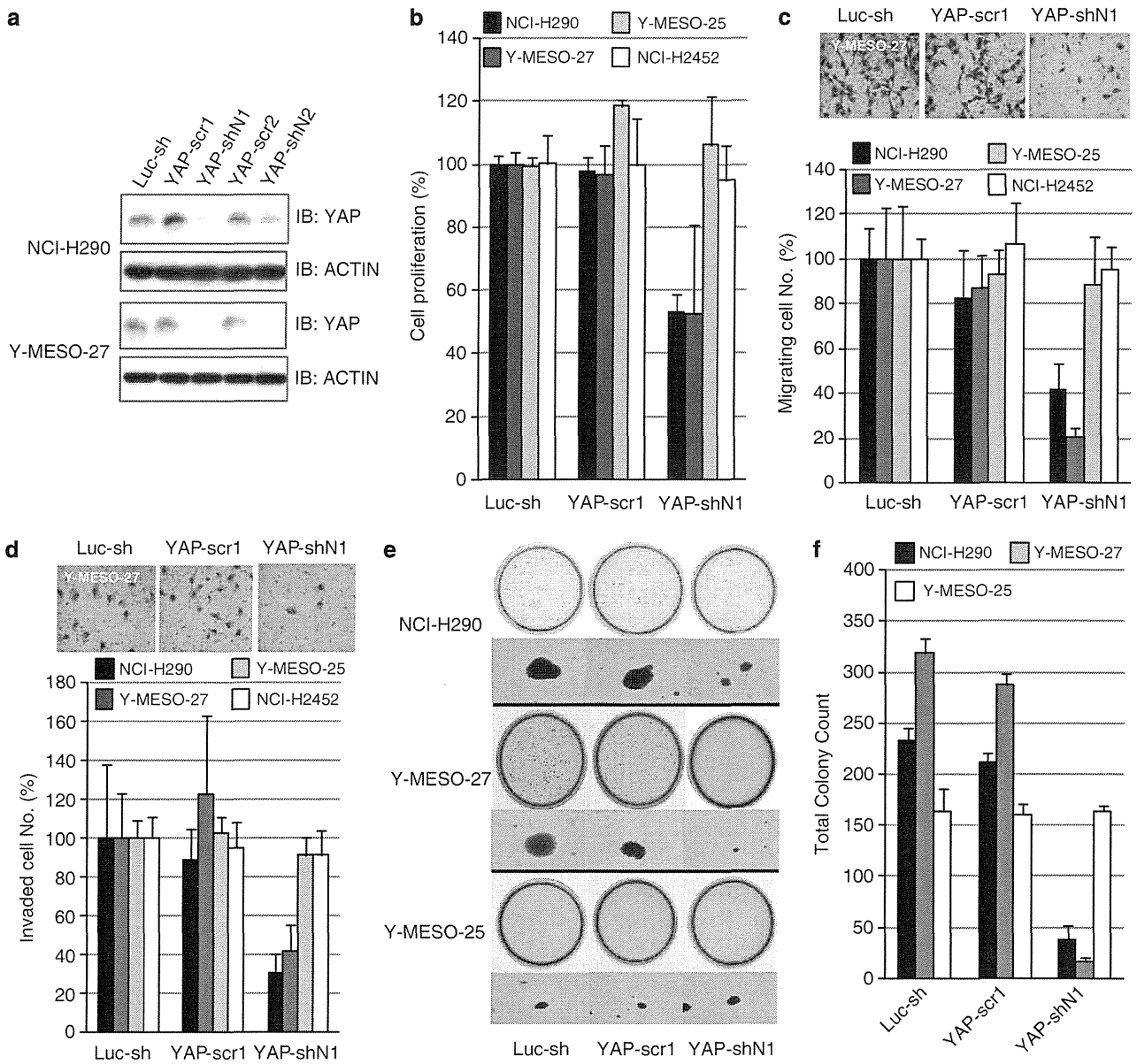

Figure 1. YAP knockdown suppressed malignant phenotypes of MM cell lines with YAP activation (NCI-H290 and Y-MESO-27) but not of those without YAP activation (Y-MESO-25 and NCI-H2452). (**a**) Western blot analyses for knockdown efficacies of short hairpin (sh)-YAP RNA interference lentivirus vectors. Two sh-YAP RNA interference lentivirus vectors (YAP-shN1 and YAP-shN2) contained each target sequence of YAP. Control shRNA vectors for luciferase (Luc-sh) with the target sequence for luciferase and for YAP (YAP-scr1 and YAP-scr2) with each scrambled target sequence were also constructed. Total cell lysates were subjected to western blot analysis using rabbit anti-YAP antibody and mouse anti-β-actin antibody. YAP-shN1 induced more potent YAP suppression compared with YAP-shN2. (**b**) Cell proliferation assay. After 72 h of lentivirus infection, calorimetric assays were performed with Tetra Color One (Seikagaku, Tokyo, Japan) and absorbance was measured at 450 nm. Cell proliferations were reduced to approximately 50% with YAP knockdown in NCI-H290 and Y-MESO-27 cell lines. (**c**) Migration assay. Cell migration and invasion potential were measured by *in vitro* Boyden chamber assays (BD Biosciences Discovery Labware, Bedford, MA, USA). Upper photographs show representative images of the migrating Y-MESO-27 cells. (**d**) Invasion assay. Matrigel matrix insert membrane was used for invasion assay. Upper photographs show representative images of invading Y-MESO-27 cells. (**e**) Soft agar colony formation assays. After a 10 day-incubation, colonies were stained with 0.3% crystal violet. Photographs of low (top) and high magnification (bottom) show that anchorage-independent growth was significantly suppressed with YAP knockdown in NCI-H290 and Y-MESO-27 but not Y-MESO-25 cell line. (**f**) A graphic presentation of the soft agar colony formation assays of (**e**). Columns are the means of experiments, and bars represent s.d. (**b**, **c**, **d**, **f**).

RESULTS AND DISCUSSION

Knockdown of YAP suppressed oncogenic properties of MM cells

We previously reported that several MM cell lines with *NF2* and/or *LATS2* mutations have constitutive YAP activation with low-level phosphorylation of YAP (S127).[16] Using western blot analysis with a panel of 23 MM cell lines, we confirmed that 16 (70%) cell lines showed lower levels of pYAP-S127 than MeT-5A, a transformed normal mesothelial cell line (Supplementary Figure 1). Among them, we selected three MM cell lines with constitutive YAP activation for further analyses; NCI-H290 with *NF2* inactivation, and Y-MESO-27 and Y-MESO-30 with *LATS2* inactivation.

Table 1. Gene ontology and pathway analyses in 228 genes commonly downregulated by YAP knockdown

Rank	*Name*	*Score*	*Score (p)*	*Score (v)*	*Score (c)*
(a) *Top 10 Gene ontology*					
1	Cell cycle (GO:0007049)	137.598	3.791E−042	0.409	0.079
2	Cell cycle process (GO:0022402)	129.250	1.235E−039	0.358	0.090
3	Cell cycle phase (GO:0022403)	117.627	3.897E−036	0.302	0.105
4	Mitotic cell cycle (GO:0000278)	107.258	5.153E−033	0.289	0.097
5	Mitotic phase (GO:0000279)	90.202	7.021E−028	0.214	0.124
6	Regulation of cell cycle (GO:0051726)	86.379	9.939E−027	0.264	0.080
7	Organelle organization (GO:0006996)	82.447	1.517E−025	0.371	0.047
8	Regulation of cell cycle process (GO:0010564)	80.848	4.596E−025	0.176	0.147
9	Regulation of metabolic process (GO:0019222)	76.863	7.275E−024	0.528	0.029
10	Regulation of cellular metabolic process (GO:0031323)	71.798	2.435E−022	0.491	0.030
(b) *Top 10 gene pathway*					
1	Transcriptional regulation by RB/E2F	297.728	2.371E−090	0.234	0.207
2	Transcriptional regulation by FOXM	63.604	7.135E−020	0.043	0.360
3	Aurora signaling pathway	52.246	1.872E−016	0.038	0.258
4	CDK signaling pathway	46.256	1.190E−014	0.043	0.107
5	PLK signaling pathway	45.168	2.531E−014	0.033	0.241
6	Transcriptional regulation by AP-1	35.712	1.777E−011	0.038	0.067
7	Nucleophosmin signaling pathway	29.087	1.753E−009	0.024	0.152
8	Wnt signaling pathway	28.376	2.870E−009	0.029	0.076
9	Transcriptional regulation by Myb	27.041	7.242E−009	0.029	0.065
10	PIN1 signaling pathway	22.329	1.898E−007	0.024	0.061

Abbreviations: AP-1, adaptor-related protein complex 1; CDK, cyclin-dependent kinase; FOXM, forkhead box M; Myb, v-myb myeloblastosis viral oncogene homolog; PIN, peptidylprolyl cis/trans isomerase NIMA-interacting 1; PLK, polo-like kinase; RB/E2F, retinoblastoma/E2F transcription factor.

As we previously showed that YAP inhibition suppressed NCI-H290 cell proliferation,[17] we first confirmed that a newly established YAP-shRNA lentivirus more efficiently suppressed the YAP expression and inhibited the cell proliferation of NCI-H290 cell line and another MM cell line, Y-MESO-27, which had *LATS2* deletion, but not in two other MM cell lines, Y-MESO-25 and NCI-H2452, without YAP activation (Figures 1a and b). Next, we analysed whether YAP knockdown affected other malignant phenotypes of MM cells *in vitro*. Both motility and invasive abilities were significantly inhibited in NCI-H290 and Y-MESO-27 cells (Figures 1c and d). Anchorage-independent growth analysis revealed a nearly complete suppression of colony formation in Y-MESO-27 cells and an 80% decrease in NCI-H290 cells (Figures 1e and f). These results indicate that YAP suppression in MM cells with constitutively activated YAP induces significant suppression of motility, invasion and anchorage-independent growth as well as cell proliferation *in vitro*.

Identification of YAP-regulating genes by microarray-based expression profiling analysis

As for the target genes of YAP orthologs, *cyclin E, Diap1* and *bantam* microRNA have been identified for *Drosophila Yokie*.[19] For mammalian YAP, although several genes including the *connective tissue growth factor* (*CTGF*) gene were shown as direct target genes of YAP,[24] other possible candidate target genes for mammalian counterparts do not seem to be really substantiated yet or even excluded, implying that YAP target genes vary among different species as well as among different cell types.

To identify the genes inducible for expression by YAP and responsible for MM cell proliferation, we performed microarray-based expression profiling analysis of the three MM cell lines after YAP knockdown. We found that 1381, 650 and 2097 genes were downregulated to equal or less than 0.5 in the NCI-H290, Y-MESO-27 and Y-MESO-30 cells, respectively, compared with each counterpart cell with the control vector (data not shown). We found that 228 genes were commonly downregulated by YAP knockdown, suggesting that this gene set includes strong candidates for YAP target genes in MM cells (Supplementary Table 1). To characterize the 228 genes, we performed gene ontology analysis and found that the large portion of YAP-regulatory genes is associated with cell cycle regulation (Table 1). Subsequent pathway analysis revealed that the pathways of transcriptional regulation by *RB/E2F* and *FOXM* were most significantly correlated (Table 1).

Meanwhile, our results revealed that 156 genes were commonly upregulated after YAP knockdown over twofold (Supplementary Table 1). Gene ontology and pathway analyses indicated that genes involved in wounding, inflammation and cell–extracellular matrix adhesion were upregulated, suggesting that suppression of these signaling pathways might also contribute to malignant phenotypes of MM cells by YAP activation, albeit their expressions might be indirectly suppressed (Supplementary Table 2).

YAP regulates CCND1 and FOXM1 transcription directly in cooperation with TEAD

Among the identified cell cycle regulatory genes, we focused on *CCND1*, a G1 cyclin-regulating RB/E2F pathway, and *FOXM1*, a transcription factor targeting both G1/S and G2/M progression regulators. *CCND1* and *FOXM1* were found to be commonly downregulated in the three cell lines from 0.13 to 0.48 and from 0.13- to 0.42-changes, respectively (Supplementary Table 1). Moreover, their promoter regions were also likely to harbor a putative recognition motif of TEAD, a transcriptional factor that binds to YAP.

To determine whether YAP regulates transcription of *CCND1* and *FOXM1* directly in MM cells, we carried out a chromatin immunoprecipitation assay. We prepared a primer set for the proximal promoter region of both genes to include the putative TEAD recognition motif[33] (Figure 2a). When precipitated with anti-YAP antibody, we detected positive PCR products of the proximal promoter regions of both genes, which indicated the direct binding of YAP to the *CCND1* and *FOXM*1 proximal promoter regions (Figure 2b), although they were not detected in the distal regions (data not shown).

Next, to determine whether YAP induces transcription of *CCND1* and *FOXM1*, and then transcription is further enhanced

by exogenous TEAD transcription factor, we performed luciferase reporter assay for the promoter regions of these genes (Figure 2a) with YAP wild type and its constitutively active form, YAP S127A. We found that cotransduction of wild-type TEAD4 with YAP wild type or the active mutant form significantly induced both *CCND1* and *FOXM1* promoter activities. On the other hand, cotransduction of other mutant forms including YAP S94A[24] or TEAD4ΔCt,[34] both of which were thought to disrupt the YAP-TEAD interaction, did not show the enhancement of luciferase activity (Figures 2c and d).

These results provided support for the notion that *CCND1* and *FOXM1* might be the direct target genes of YAP in MM cells. Consistent with our observations, induction of *CCND1* by YAP has also been suggested by other studies. For example, in vertebrate neural tube development, YAP and TEAD promoted cell cycle progression by inducing *CCND1*.[21] As an upstream suppressive regulator of YAP, Merlin was also shown to inhibit *CCND1* expression by using *NF2*-deficient MM cells.[35] Although those reports did not refer to transcriptional regulation of *CCND1* by YAP, they demonstrated a contribution of Hippo signaling pathway to *CCND1* regulation, which our present findings corroborate.

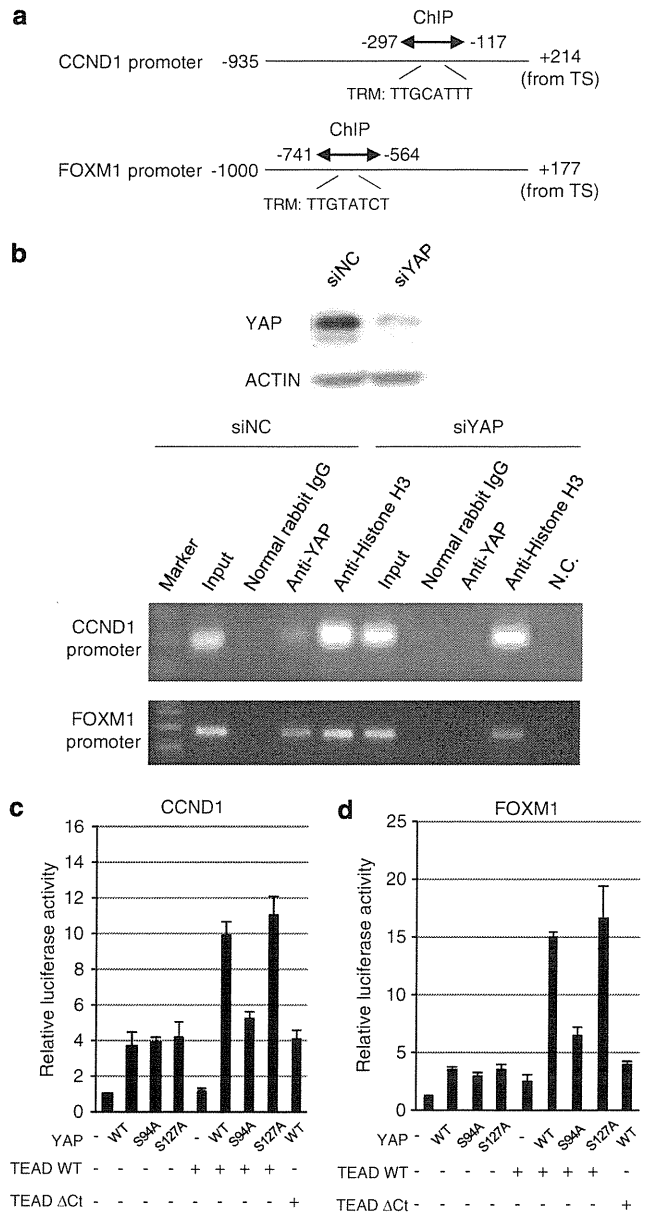

Figure 2. YAP directly induces transcription of the *CCND1* and *FOXM1* genes. (**a**) Each promoter includes the putative TEAD recognition motif (TRM), XDGHATXT, where X = A, T, C or G; D = A or T; and H = A, T or C. ChIP primer sets (arrow) were designed to include the motif. DNA fragments of nucleotide position −935 to +214 for *CCND1* and nucleotide position −1000 to +177 for *FOXM1* were inserted into luciferase reporter vectors. TS: transcriptional start. (**b**) ChIP assay using ChIP kit (ab500, Abcam) demonstrated that YAP bound to the *CCND1* and *FOXM1* proximal promoter regions. NCI-H290 cells treated with YAP siRNA (siYAP; Ambion, Austin, TX) were used as YAP-suppressed control, while cells with an irrelevant siRNA (siNC) maintained high YAP expression, as confirmed with western blot analysis. (Upper panel) After the cells with high or low YAP expression were subjected to immunoprecipitation assay with normal rabbit IgG (SC2027, Santa Cruz), rabbit anti-YAP antibody, or anti-H3 antibody (ab1791, Abcam) and protein A beads, immunoprecipitated chromatin were decross-linked. Recruited DNA was subjected to PCR using primer sets for proximal promoter regions of *CCND1* and *FOXM1*, and PCR products were electrophoresed in agarose gel. (Lower panel) Note that amounts of PCR products from the chromatin, which was precipitated with the anti-YAP antibody, were suppressed by pretreatment with siYAP. (**c, d**) For reporter assay, MeT-5A cells were transfected with the pGL3 basic firefly luciferase reporter plasmid with the *CCND1* or *FOXM1* promoter region by using FuGENE 6 transfection reagent (Roche, Mannheim, Germany). Renilla luciferase plasmid was also transfected for internal control. Thirty-six hours later, cells were lysed and subjected to dual-luciferase assay (TOYO INK, Tokyo, Japan). The promoter activities were enhanced with combined transduction of TEAD4 WT with wild type (WT) or constitutively activated forms of YAP (YAP S127A), but not with YAP S94A (inactive for TEAD binding) or TEAD4ΔCt (inactive for YAP binding) forms. Columns are the means of experiments, and bars represent s.d. (**c, d**).

YAP depletion suppressed cell cycle-promoting gene expressions in MM cells

The gene ontology analysis based on the microarray-based expression profiling suggested a significant contribution of YAP to the cell cycle process in MM cells. Based on our previous data indicating G1 cell cycle arrest in NCI-H290 cells by YAP knockdown,[17] we studied the status of cell cycle and expressions of cell cycle-promoting genes in a time-dependent manner after YAP-shRNA lentivirus infection. We found that G1 cell cycle arrest occurred at as early as 48 h, and the population of G1 cell cycle arrest increased at 72 h (Figure 3a). With quantitative real-time RT-PCR analysis, suppression of the *CCND1* gene expression was revealed to follow the downregulation of *YAP* as expected (Figure 3c). Consistent with the expression array analysis, other cell cycle-promoting genes including *E2F1*, *Aurora kinase B* (*AURKB*), *Polo-like kinase 1* (*PLK1*) and *NIMA-related kinase 2* (*NEK2*), also showed the decrease in the expression levels according to YAP-downregulation (Figure 3c). However, other irrelevant genes such as *SMAD3* did not show any decrease (data not shown). These results suggested that, together with YAP-direct target genes of *CCND1* and *FOXM1*, other cell-promoting genes are also involved in the dysregulated cell cycle machinery in YAP-activated MM cells.

Additionally, we observed that YAP-knockdown increased subG1 population of the cells in flow cytometric analysis (Figure 3b) and affected the expression levels of several apoptotic-related genes, including the downregulation of *BIRC5* (also known as *survivin*), an anti-apoptotic gene, and upregulated the one of *BCL2L11* (also known as *BIM*), a pro-apoptotic gene (Supplementary Table 2). In a flow cytometric assay with

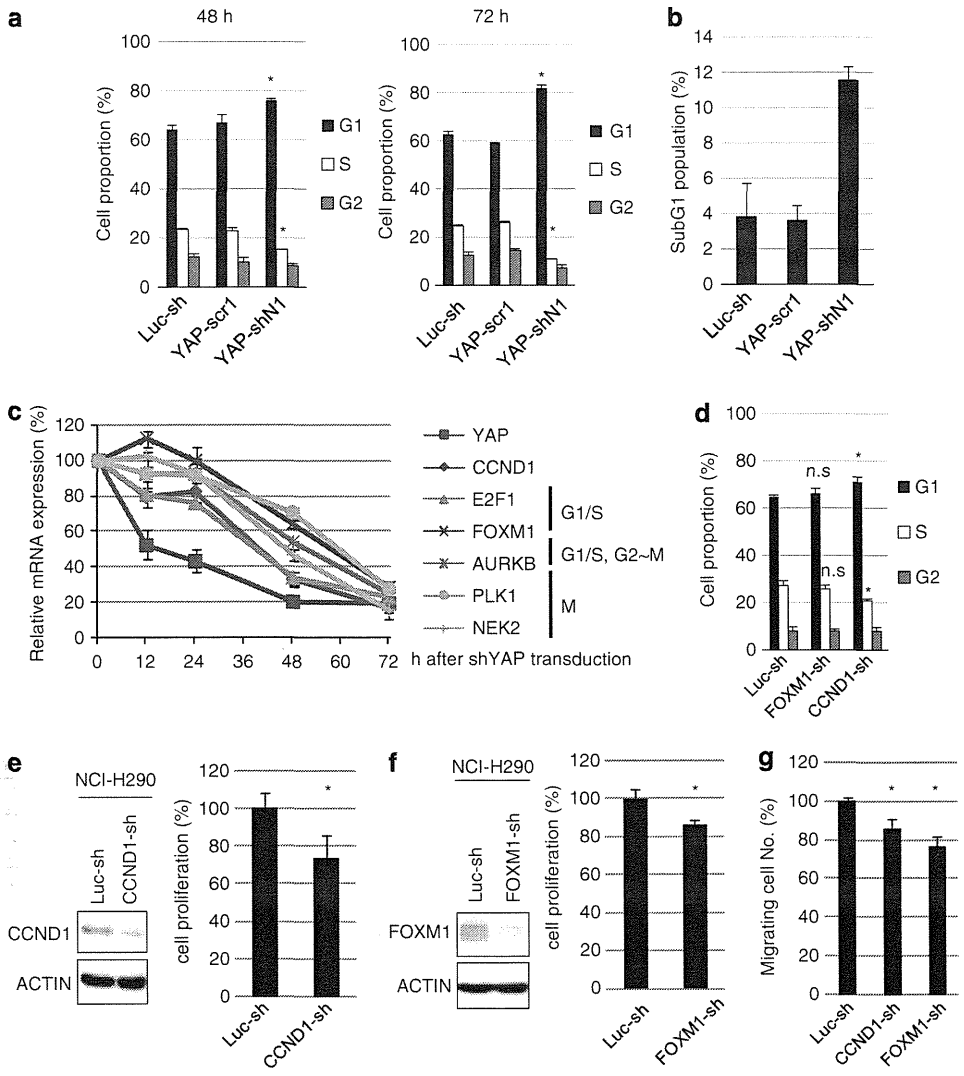

Figure 3. Involvement of YAP, CCND1 and FOXM1 in cell proliferation in NCI-H290 cells. (**a**) Flow cytometry analysis. After infection with YAP-shN1, YAP-scr1, or Luc-sh lentivirus, cells were incubated to grow for 48 or 72 h. Cells were harvested, washed with PBS and fixed with 70% ethanol. After treatment by RNaseA, cells were stained with propidium iodide (Sigma) and flow cytometry analysis was carried out. Cell cycle analysis revealed increased population of G1 phase and decreased population of S phase in NCI-H290 cells 48 h (left) and 72 h (right), respectively, after YAP-shN1 lentivirus infection. (**b**) YAP-knockdown induced subG1 population of MM cells. (**c**) Quantitative real-time RT-PCR analysis was performed with ABI 7500 Real-Time PCR System (Applied Biosystems, Foster, CA, USA). Glyceraldehyde-3-phosphate dehydrogenase (GAPDH) served as an endogenous control. The graph shows the changes in mRNA expression levels of cell cycle-related genes in response to YAP depletion. Symbols are the means of experiments normalized to control cell, and bars represent s.d. (**d**) Flow cytometry analysis. Knockdown of *CCND1* modestly increased the number of G1/S arrest cells in MM cells. (**e**, **f**) Cell proliferation assay. Knockdown of *CCND1* (**e**) and *FOXM1* (**f**) moderately suppressed cell proliferation in NCI-H290 cells. (**g**) Cell migration assay. Knockdown of *CCND1* and *FOXM1* induced modest suppression of NCI-H290 cell migratory activity. Columns are the means of experiments, and bars represent s.d. Asterisks represent $P<0.05$ between YAP-shN1 (**a**), CCND1-sh (**d**, **e**, **g**), or FOXM1-sh (**d**, **f**, **g**) versus Luc-sh control. n.s., not significant.

annexin V, a modest increase of early apoptotic cell population was also detected (Supplementary Figure 2). Although these data suggested apoptosis induction in MM cells, we did not find significant caspase activation with western blot analysis probably due to a relatively small population of MM cells that underwent apoptosis (data not shown). Thus, further studies may be warranted to clarify the underlying mechanism and significance of cell death by YAP-knockdown in MM cells.

CCND1 contributes to G1/S transition in MM cells

To determine whether knockdown of individual cell cycle specific genes regulated by YAP is sufficient to induce G1 cell cycle arrest in MM cells, we performed cell cycle analysis of NCI-H290 cells with knockdown of *CCND1* or *FOXM1*. After transduction of CCND1-sh, we found that the cell population of G1 phase increased and that of S phase decreased compared with the control cell (Figure 3d), although the effect was weaker than that of YAP-sh. However, the effect of FOXM1-sh on cell cycle progression was not clear (Figure 3d).

Finally, to evaluate proliferative roles of CCND1 or FOXM1 as YAP transcriptional targets in MM cells, we knocked down *CCND1* and *FOXM1* and performed proliferation analysis. The depletion of CCND1 and FOXM1 caused modest suppression compared with YAP depletion, though the decrease of proliferation was larger in CCND1 depletion than FOXM1 depletion at 26% and 14%,

respectively (Figures 3e and f). Taken together, these results suggested that YAP contributes to expression of a wide range of cell cycle-promoting genes and induces MM cell proliferation, although knockdown of individual YAP target genes shows moderate effects.

In conclusion, we showed that YAP induces multiple gene expression, which includes cell cycle-promoting genes such as *CCND1* and *FOXM1* in MM cells. Our findings thus serve to elucidate some important aspects of dysregulated cell cycle control mechanisms in MM cells through YAP activation. As individual inhibition of YAP target genes did not suppress MM proliferation sufficiently, we speculate that a wide range of genes evoked by YAP activation induce MM cell proliferation and progression as a whole. Thus, our results suggest that YAP itself may be a key target molecule for the development of a new molecular target therapy for MM.

CONFLICT OF INTEREST

The authors declare no conflict of interest.

ACKNOWLEDGEMENTS

We thank Ms Mika Yamamoto for her excellent technical assistance. This work was supported in part by a Special Coordination Fund for Promoting Science and Technology from the Ministry of Education, Culture, Sports, Science and Technology of Japan (H18-1-3-3-1), KAKENHI (18390245, 22300338), Grant-in-Aid for Third-Term Comprehensive Control Research for Cancer from the Ministry of Health, Labor and Welfare of Japan, the Takeda Science Foundation and the Kobayashi Foundation for Cancer Research.

REFERENCES

1 Pass HI, Vogelzang N, Hahn S, Carbone M. Malignant pleural mesothelioma. *Curr Probl Cancer* 2004; **28**: 93 - 174.
2 Yang H, Testa JR, Carbone M. Mesothelioma epidemiology, carcinogenesis, and pathogenesis. *Curr Treat Options Oncol* 2008; **9**: 147 - 157.
3 Robinson BW, Lake RA. Advances in malignant mesothelioma. *N Engl J Med* 2005; **353**: 1591 - 1603.
4 Vogelzang NJ, Rusthoven JJ, Symanowski J, Denham C, Kaukel E, Ruffie P *et al.* Phase III study of pemetrexed in combination with cisplatin versus cisplatin alone in patients with malignant pleural mesothelioma. *J Clin Oncol* 2003; **21**: 2636 - 2644.
5 Carbone M, Kratzke RA, Testa JR. The pathogenesis of mesothelioma. *Semin Oncol* 2002; **29**: 2 - 17.
6 Sekido Y. Genomic abnormalities and signal transduction dysregulation in malignant mesothelioma cells. *Cancer Sci* 2010; **101**: 1 - 6.
7 Illei PB, Ladanyi M, Rusch VW, Zakowski MF. The use of CDKN2A deletion as a diagnostic marker for malignant mesothelioma in body cavity effusions. *Cancer* 2003; **99**: 51 - 56.
8 Bianchi AB, Mitsunaga SI, Cheng JQ, Klein WM, Jhanwar SC, Seizinger B *et al.* High frequency of inactivating mutations in the neurofibromatosis type 2 gene (NF2) in primary malignant mesotheliomas. *Proc Natl Acad Sci USA* 1995; **92**: 10854 - 10858.
9 Sekido Y, Pass HI, Bader S, Mew DJ, Christman MF, Gazdar AF *et al.* Neurofibromatosis type 2 (NF2) gene is somatically mutated in mesothelioma but not in lung cancer. *Cancer Res* 1995; **55**: 1227 - 1231.
10 Bott M, Brevet M, Taylor BS, Shimizu S, Ito T, Wang L *et al.* The nuclear deubiquitinase BAP1 is commonly inactivated by somatic mutations and 3p21.1 losses in malignant pleural mesothelioma. *Nat Genet* 2011; **43**: 668 - 672.
11 Testa JR, Cheung M, Pei J, Below JE, Tan Y, Sementino E *et al.* Germline BAP1 mutations predispose to malignant mesothelioma. *Nat Genet* 2011; **43**: 1022 - 1025.
12 Hamaratoglu F, Willecke M, Kango-Singh M, Nolo R, Hyun E, Tao C *et al.* The tumour-suppressor genes NF2/Merlin and expanded act through Hippo signalling to regulate cell proliferation and apoptosis. *Nat Cell Biol* 2006; **8**: 27 - 36.
13 Dong J, Feldmann G, Huang J, Wu S, Zhang N, Comerford SA *et al.* Elucidation of a universal size-control mechanism in Drosophila and mammals. *Cell* 2007; **130**: 1120 - 1133.
14 Saucedo LJ, Edgar BA. Filling out the Hippo pathway. *Nat Rev Mol Cell Biol* 2007; **8**: 613 - 621.
15 Zhang N, Bai H, David KK, Dong J, Zheng Y, Cai J *et al.* The Merlin/NF2 tumor suppressor functions through the YAP oncoprotein to regulate tissue homeostasis in mammals. *Dev Cell* 2010; **19**: 27 - 38.
16 Murakami H, Mizuno T, Taniguchi T, Fujii M, Ishiguro F, Fukui T *et al.* LATS2 is a tumor suppressor gene of malignant mesothelioma. *Cancer Res* 2011; **71**: 873 - 883.
17 Yokoyama T, Osada H, Murakami H, Tatematsu Y, Taniguchi T, Kondo Y *et al.* YAP1 is involved in mesothelioma development and negatively regulated by Merlin through phosphorylation. *Carcinogenesis* 2008; **29**: 2139 - 2146.
18 Sekido Y. Inactivation of Merlin in malignant mesothelioma cells and the Hippo signaling cascade dysregulation. *Pathol Int* 2011; **61**: 331 - 344.
19 Huang J, Wu S, Barrera J, Matthews K, Pan D. The Hippo signaling pathway coordinately regulates cell proliferation and apoptosis by inactivating Yorkie, the Drosophila homolog of YAP. *Cell* 2005; **122**: 421 - 434.
20 Tapon N, Harvey KF, Bell DW, Wahrer DC, Schiripo TA, Haber DA *et al.* Salvador promotes both cell cycle exit and apoptosis in Drosophila and is mutated in human cancer cell lines. *Cell* 2002; **110**: 467 - 478.
21 Cao X, Pfaff SL, Gage FH. YAP regulates neural progenitor cell number via the TEA domain transcription factor. *Genes Dev* 2008; **22**: 3320 - 3334.
22 Nishioka N, Inoue K, Adachi K, Kiyonari H, Ota M, Ralston A *et al.* The Hippo signaling pathway components Lats and Yap pattern Tead4 activity to distinguish mouse trophectoderm from inner cell mass. *Dev Cell* 2009; **16**: 398 - 410.
23 Zhang X, Milton CC, Humbert PO, Harvey KF. Transcriptional output of the Salvador/Warts/Hippo pathway is controlled in distinct fashions in Drosophila melanogaster and mammalian cell lines. *Cancer Res* 2009; **69**: 6033 - 6041.
24 Zhao B, Ye X, Yu J, Li L, Li W, Li S *et al.* TEAD mediates YAP-dependent gene induction and growth control. *Genes Dev* 2008; **22**: 1962 - 1971.
25 Hall CA, Wang R, Miao J, Oliva E, Shen X, Wheeler T *et al.* Hippo pathway effector Yap is an ovarian cancer oncogene. *Cancer Res* 2010; **70**: 8517 - 8525.
26 Muramatsu T, Imoto I, Matsui T, Kozaki K, Haruki S, Sudol M *et al.* YAP is a candidate oncogene for esophageal squamous cell carcinoma. *Carcinogenesis* 2011; **32**: 389 - 398.
27 Wang Y, Dong Q, Zhang Q, Li Z, Wang E, Qiu X. Overexpression of yes-associated protein contributes to progression and poor prognosis of non-small-cell lung cancer. *Cancer Sci* 2010; **101**: 1279 - 1285.
28 Xu MZ, Yao TJ, Lee NP, Ng IO, Chan YT, Zender L *et al.* Yes-associated protein is an independent prognostic marker in hepatocellular carcinoma. *Cancer* 2009; **115**: 4576 - 4585.
29 Zhang X, George J, Deb S, Degoutin JL, Takano EA, Fox SB *et al.* The Hippo pathway transcriptional co-activator, YAP, is an ovarian cancer oncogene. *Oncogene* 2011; **30**: 2810 - 2822.
30 Basu S, Totty NF, Irwin MS, Sudol M, Downward J. Akt phosphorylates the Yes-associated protein, YAP, to induce interaction with 14-3-3 and attenuation of p73-mediated apoptosis. *Mol Cell* 2003; **11**: 11 - 23.
31 Lapi E, Di Agostino S, Donzelli S, Gal H, Domany E, Rechavi G *et al.* PML, YAP, and p73 are components of a proapoptotic autoregulatory feedback loop. *Mol Cell* 2008; **32**: 803 - 814.
32 Levy D, Adamovich Y, Reuven N, Shaul Y. The Yes-associated protein 1 stabilizes p73 by preventing Itch-mediated ubiquitination of p73. *Cell Death Differ* 2007; **14**: 743 - 751.
33 Anbanandam A, Albarado DC, Nguyen CT, Halder G, Gao X, Veeraraghavan S. Insights into transcription enhancer factor 1 (TEF-1) activity from the solution structure of the TEA domain. *Proc Natl Acad Sci USA* 2006; **103**: 17225 - 17230.
34 Vassilev A, Kaneko KJ, Shu H, Zhao Y, DePamphilis ML. TEAD/TEF transcription factors utilize the activation domain of YAP65, a Src/Yes-associated protein localized in the cytoplasm. *Genes Dev* 2001; **15**: 1229 - 1241.
35 Xiao GH, Gallagher R, Shetler J, Skele K, Altomare DA, Pestell RG *et al.* The NF2 tumor suppressor gene product, merlin, inhibits cell proliferation and cell cycle progression by repressing cyclin D1 expression. *Mol Cell Biol* 2005; **25**: 2384 - 2394.

Supplementary Information accompanies the paper on the Oncogene website (http://www.nature.com/onc)

Carcinogenesis vol.33 no.7 pp.1277–1285, 2012
doi:10.1093/carcin/bgs154
Advance Access publication April 24, 2012

Integrated analysis of genetic and epigenetic alterations reveals CpG island methylator phenotype associated with distinct clinical characters of lung adenocarcinoma

Keiko Shinjo[1,2], Yasuyuki Okamoto[1], Byonggu An[1], Toshihiko Yokoyama[3], Ichiro Takeuchi[4], Makiko Fujii[1], Hirotaka Osada[1,2], Noriyasu Usami[5], Yoshinori Hasegawa[3], Hidemi Ito[6], Toyoaki Hida[7], Nobukazu Fujimoto[8], Takumi Kishimoto[8], Yoshitaka Sekido[1,2] and Yutaka Kondo[1,9,*]

[1]Division of Molecular Oncology, Aichi Cancer Center Research Institute, 1-1 Kanokoden, Chikusa-ku, Nagoya 464-8681, Japan, [2]Department of Cancer Genetics, [3]Department of Respiratory Medicine, Nagoya University Graduate School of Medicine, Nagoya, Japan, [4]Graduate School of Engineering, Nagoya Institute of Technology, Nagoya, Japan, [5]Division of General Thoracic Surgery, Nagoya University Graduate School of Medicine, Nagoya, Japan, [6]Division of Epidemiology and Prevention, Aichi Cancer Center Research Institute, Nagoya, Japan, [7]Department of Thoracic Oncology, Aichi Cancer Center Hospital, Nagoya, Japan, [8]Department of Respiratory Medicine, Okayama Rosai Hospital, Okayama, Japan and [9]Precursory Research for Embryonic Science and Technology (PRESTO), Japan Science and Technology Agency, Saitama, Japan

*To whom correspondence should be addressed. Tel: +81 52 764 2994; Fax: +81 52 764 2994;
Email: ykondo@aichi-cc.jp

DNA methylation affects the aggressiveness of human malignancies. Cancers with CpG island methylator phenotype (CIMP), a distinct group with extensive DNA methylation, show characteristic features in several types of tumors. In this study, we initially defined the existence of CIMP in 41 lung adenocarcinomas (AdCas) through genome-wide DNA methylation microarray analysis. DNA methylation status of six CIMP markers newly identified by microarray analysis was further estimated in a total of 128 AdCas by bisulfite pyrosequencing analysis, which revealed that 10 (7.8%), 40 (31.3%) and 78 (60.9%) cases were classified as CIMP-high (CIMP-H), CIMP-low and CIMP-negative (CIMP-N), respectively. Notably, CIMP-H AdCas were strongly associated with wild-type epidermal growth factor receptor (*EGFR*), males and heavy smokers ($P = 0.0089$, $P = 0.0047$ and $P = 0.0036$, respectively). In addition, CIMP-H was significantly associated with worse prognosis; especially among male smokers, CIMP-H was an independent prognostic factor (hazard ratio 1.7617, 95% confidence interval 1.0030–2.9550, $P = 0.0489$). Compellingly, the existence of CIMP in AdCas was supported by the available public datasets, such as data from the Cancer Genome Atlas. Intriguingly, analysis of AdCa cell lines revealed that CIMP-positive AdCa cell lines were more sensitive to a DNA methylation inhibitor than CIMP-N ones regardless of *EGFR* mutation status. Our data demonstrate that CIMP in AdCas appears to be a unique subgroup that has distinct clinical traits from other AdCas. CIMP classification using our six-marker panel has implications for personalized medical strategies for lung cancer patients; in particular, DNA methylation inhibitor might be of therapeutic benefit to patients with CIMP-positive tumors.

Introduction

Lung cancer is the leading cause of human cancer death worldwide (1). Recent targeted therapies have improved the survival of patients with certain types of lung cancer, especially adenocarcinoma (AdCa), a common type of non-small cell lung cancer. AdCas with epidermal growth factor receptor (*EGFR*) mutation benefit particularly from EGFR tyrosine kinase inhibitors (TKIs) (2), whereas those harboring *EML4–ALK* fusion are highly sensitive to anaplastic lymphoma kinase (ALK) inhibitors (3). Despite these recent advances in targeted therapy for AdCas, a considerable number of patients with lung cancer still suffer from recurrence of disease. AdCas without such mutations are generally less sensitive to these targeted therapies than tumors with mutations. Given the evidence that the frequency of *EGFR* mutations account for up to 30% of AdCas, and even *EML4–ALK* fusions are found in AdCas albeit at a lower frequency, elucidating the underlying mechanisms other than such gene alterations in lung carcinogenesis is desirable to facilitate the development of new strategies for lung cancer treatment.

Studies have shown that in addition to genetic alterations, accumulation of epigenetic alterations play an important role in tumorigenesis of lung cancer (4). DNA methylation, an important epigenetic factor, affects the chromatin structure and is closely associated with gene regulation (5). Simultaneous dysregulation of multiple genes, including those involved in cell cycle, cell growth, cell death or cell adhesion, by DNA methylation may be a strong driving force to undergo transformation, sometimes in correlation with potentiated aggressiveness of the tumors (6).

Recent studies in colon cancer have shown that a subset of tumors suffer from a remarkably high rate of aberrant promoter DNA methylation at a large number of loci, referred to as CpG island methylator phenotype (CIMP) (7). CIMP tumors in colon exhibit distinct genetic and clinical features, such as high rates of *BRAF* and *KRAS* mutations, low frequency of *TP53* mutation, specific histology, proximal location and characteristic clinical outcome, suggesting that CIMP-related cancers may proceed through a unique pathway (8). In lung cancer, some studies have shown the existence of a subgroup of tumors with the characteristic methylation status of CIMP (9–13). However, in comparison with the considerable research of CIMP markers performed in colon cancers (7,14–16), no studies have assessed which DNA methylation markers can predict the most extensively methylated subgroups (i.e. CIMP) in lung AdCas due to the lack of accompanied genome-wide DNA methylation analysis in multiple samples. Since different panels of markers may lead to different classification of lung cancer (9,11), it is important to define markers that can accurately identify CIMP.

To examine whether CIMP exists as a characteristic subgroup in AdCas, we initially performed global screening for genes with aberrant DNA hypermethylation by the methylated CpG island amplification microarray (MCAM) analysis, which provides reproducible results with a high validation rate (16–20). Using the six CIMP markers newly identified by MCAM analysis, we characterized a distinct subgroup of AdCas exhibiting CIMP. In addition, several AdCa cell lines with different CIMP status were treated with a DNA methylation inhibitor, and the relationship between DNA methylation status and drug sensitivity was assessed. Our data provide evidence for a new strategy for lung cancer treatment.

Abbreviations: AdCa, adenocarcinoma; CIMP, CpG island methylator phenotype; CIMP-H, CIMP-high; CIMP-L, CIMP-low; CIMP-N, CIMP-negative; EGFR, epidermal growth factor receptor; MCAM, methylated CpG island amplification microarray; TCGA, the cancer genome atlas; TKI, tyrosine kinase inhibitor;

Materials and methods

Cell lines

A549 was purchased from the American Type Culture Collection (Rockville, MD) and PC9 was purchased from Immuno-Biological Laboratories (Fujioka, Gunma, Japan). NCI-H23, NCI-H358, NCI-H920, NCI-H2009, NCI-H1573, NCI-H1650 and HCC4011 were kind gifts from Dr Adi F. Gazdar (University of Texas Southwestern Medical Center, Dallas, TX) and Dr Mitsuo Sato (Nagoya University Graduate School of Medicine, Nagoya, Japan). Y-ML13 (ML13) and ACC-H1 (H1) were established in our institute. All cell lines were maintained in RPMI-1640 medium (Sigma–Aldrich, St Louis, MO) supplemented with 10%

fetal bovine serum (Invitrogen, Carlsbad, CA) and antibiotic–antimycotic reagent (Invitrogen) at 37°C in a humidified incubator with 5% CO_2.

5-Aza-dC treatment of cells

Cells were treated with 50 nM–1 μM 5-aza-2′-deoxycytidine (5-Aza-dC; Sigma–Aldrich) as described previously (17) or the TKI AG1478 (Calbiochem, San Diego, CA) for 72 h. DNA was extracted on the seventh day following treatment. Changes in proliferation were determined by using the TetraColor ONE (Seikagaku, Tokyo, Japan) system, containing 2-(2-methoxy-4-nitrophenyl)-3-(4-nitrophenyl)-5-(2,4-disulfophenyl)-2H-tetrazolium, monosodium salt and 1-methoxy-5-methylphenazinium methylsulfate as the electron carrier. After 1 h incubation at 37°C, absorbance was read at 450 nm with a multiplate reader. Growth inhibition was expressed as a mean ratio of absorbance reading from treated versus untreated cells. Cell numbers were also counted under a light microscope at the same time point.

Tissue samples

We collected 128 AdCa samples and 26 normal lung tissues from patients who underwent surgical resection at the Aichi Cancer Center Central Hospital, Okayama Rosai Hospital, Nagoya University Hospital and its affiliated hospitals in Japan, in accordance with the institutional policy. Samples and clinical data were collected after appropriate institutional review board approval was received and written informed consent had been obtained from all the patients. Histological and cytological examination of normal lung tissues, which were obtained from the lung cancer patients, revealed no remarkable findings as malignant tissues. In the normal tissues, no aberrant methylation was detected in 10 genes by pyrosequencing analysis (Supplementary Table 1, available at *Carcinogenesis* Online). A sample size of 124 patients was calculated to be sufficient to provide a survival rate difference of 25% with a significance level of 0.05 and power of 80%, when the frequency of CIMP-AdCa was estimated to be ~20% as is observed in colorectal cancer (8); therefore, we collected 128 AdCas to analyze the significance of CIMP (Table I).

DNA preparation

Genomic DNA was extracted using a standard phenol–chloroform method. Fully methylated DNA was prepared by treating genomic DNA with *Sss*I methylase (New England Biolabs, Ipswich, MA), and unmethylated DNA was prepared by treating genomic DNA with phi29 DNA polymerase (Genomi-Phi DNA Amplification Kit; Amersham Biosciences, Uppsala, Sweden) according to the manufacturers' protocol.

DNA methylation analysis

We performed bisulfite treatment as described previously (21,22).The DNA methylation levels were measured using pyrosequencing technology (Pyrosequencing AB, Uppsala, Sweden). Primer sequences and polymerase chain reaction conditions are shown in Supplementary Table 2, available at *Carcinogenesis* Online. All the primers were designed to examine the methylation status of CpGs within 0.5 kb of the transcription start site. A methylation level >15% was considered methylation positive since lower values could not be easily distinguished from background (17–20).

Methylated CpG island amplification microarray

For MCAM analysis, we randomly selected 41 cases from the 128 AdCas without any bias (average age was 61.9 years, ranging from 36 to 83 years old; Table I). A detailed protocol of MCA has been described previously (16–20). Briefly, amplicons from individual AdCas were labeled with Cy5 dye and cohybridized against amplicons from normal controls labeled with Cy3 dye on 15 K custom-promoter microarrays from Agilent Technologies (G4497A; Agilent Technologies, Santa Clara, CA) containing 6157 unique genes, which we had initially validated in a previous study (17). A Cy5/Cy3 signal in excess of 2.0 in MCAM was considered methylation positive (17–19). Comparison of the MCAM signal ratio (Cy5/Cy3 > 2.0 or Cy5/Cy5 ≤ 2.0) with the methylation status (positive or negative) from the pyrosequencing analysis showed a good concordance between the two analyses (sensitivity, 68.0% and specificity, 88.7%; Supplementary Table 3, available at *Carcinogenesis* Online).

Hierarchical clustering analysis

Cluster analysis was performed using an agglomerative hierarchical clustering algorithm (18,23). For specimen clustering, pairwise similarity measures among specimens were calculated using the Cluster 3.0 software (http://rana.lbl.gov/EisenSoftware.htm) or Minitab 15 statistical software (http://www.minitab.com), based on the DNA methylation intensity measurements

Table I. Clinical and molecular features according to the CIMP status

	All cases (%)	CIMP-N (%)	CIMP-L (%)	CIMP-H (%)	*P* value
Cases	128 (100)	78 (60.9)	40 (31.3)	10 (7.8)	
Age (mean ± SD)	64.7 ± 9.8	63.9 ± 10.0	66.4 ± 9.8	63.8 ± 7.0	0.4043
Gender					
Male	71 (55.5)	35 (44.9)	27 (67.5)	9 (90.0)	0.0047
Female	57 (44.5)	43 (55.1)	13 (32.5)	1 (10.0)	
Stage[a]					
I	75 (59.5)	51 (67.1)	21 (52.5)	3 (30.0)	0.2259
II	19 (15.1)	7 (9.2)	8 (20.0)	3 (30.0)	
III	29 (23.0)	16 (21.1)	10 (25.0)	4 (40.0)	
IV	3 (2.4)	2 (2.6)	1 (2.5)	0 (0)	
Smoking status					
Heavy smoker	41 (32.3)	21 (27.6)	12 (30.8)	8 (80.0)	0.0036
Light smoker	29 (22.8)	15 (19.7)	13 (33.3)	1 (10.0)	
Never-smoker	57 (44.9)	42 (55.3)	14 (35.9)	1 (10.0)	
Differentiation[a]					
Well	15 (17.4)	11 (21.2)	3 (10.7)	1 (16.7)	0.3552
Moderate	55 (64.0)	30 (57.6)	22 (78.6)	3 (50.0)	
Poorly	16 (18.6)	11 (21.2)	3 (10.7)	2 (33.3)	
Recurrence[a]					
(−)	41 (42.3)	27 (43.5)	14 (46.7)	0 (0)	0.1394
(+)	56 (57.7)	35 (56.5)	16 (53.3)	5 (100)	
EGFR mutation					
(−)	80 (62.5)	42 (53.8)	28 (70.0)	10 (100)	0.0089
(+)	48 (37.5)	36 (46.2)	12 (30.0)	0 (0)	
KRAS mutation					
(−)	118 (92.2)	74 (94.9)	36 (90.0)	8 (80.0)	0.2113
(+)	10 (7.8)	4 (5.1)	4 (10.0)	2 (20.0)	
p53 mutation[a]					
(−)	89 (69.5)	57 (74.0)	28 (73.7)	4 (40.0)	0.16
(+)	35 (27.3)	20 (26.0)	10 (26.3)	5 (50.0)	
BRAF mutation					
(−)	86 (100)	56 (100)	23 (100)	7 (100)	NA
(+)	0 (0)	0 (0)	0 (0)	0 (0)	

[a]Data were not available in some cases. Recurrence was observed within 5 years after surgery.

across all genes. *K*-means consensus clustering was performed with the R statistical package. A dendrogram and heat map were constructed using either TreeView (http://rana.lbl.gov/EisenSoftware.htm) or R statistical computing environment (http://cran.r-project.org).

Nearest neighbor classification

Using the DNA methylation status of six CIMP markers (positive or negative by pyrosequencing analysis), nearest neighbor classification was employed to classify the validation set consisting of 87 independent AdCas (24). In this analysis, each validation case was classified into one of the three clusters identified in the training set. The number of nearest neighbors was set as $k = 4$ because the smallest cluster (cluster 1) was consisted of four cases. The analysis was conducted using R statistical computing environment (http://cran.r-project.org).

Mutation analysis

Mutations in *KRAS* (codons 12 and 13) were analyzed by direct sequencing and the pyrosequencing method (25,26). *EGFR* mutations (exons 18–21) and *TP53* mutations (exons 5–8) were examined using direct sequencing (19,25). Mutation of *BRAF* (codon 600) was determined by the pyrosequencing method as previously reported (27). The polymerase chain reaction primer sequences used are listed in Supplementary Table 2, available at *Carcinogenesis* Online.

The Cancer Genome Atlas data

We obtained the methylation data of AdCa samples from the The Cancer Genome Atlas data (TCGA) web site (http://tcga-data.nci.nih.gov/tcga/tcgaHome2.jsp), and data of 85 AdCa samples (batches 34 and 37) were included in the analysis, which was conducted using the Illumina Infinium Human DNA Methylation 27 platform. The 3833 most variant probes from 27 578 CpG dinucleotides were used for further analysis, and a β value > 0.4 was considered as methylation positive.

Statistical analysis for clinical features

All statistical analyses were performed using the JMP statistical software version 5.1 (SAS Institute, Cary, NC). Fisher's exact test was used to determine non-random associations between two categorical variables. Kruskal–Wallis analysis was used to evaluate the extent of differences among more than three groups. All reported *P* values are two sided, with $P < 0.05$ taken as statistically significant. Patients were followed until incidence of death or until October 2010, whichever came first. Survival information was available for 118 of the 128 cases. Overall survival was calculated from the date of surgery until the date of death or the date the patient was last known to be alive (censored). The median follow-up time was 42.5 months. Overall survival curves were generated via the Kaplan–Meier method, and the log-rank test was used for statistical analysis. A multivariate analysis using the Cox proportional hazards model was performed to estimate the hazard ratio. All variables for the multivariate analysis were categorical variables (age, stage and CIMP status).

Results

Identification of a distinct subgroup with characteristic DNA methylation profiling in AdCas

First, we evaluated the genome-wide DNA methylation status in a training set of 41 AdCas using MCAM analysis (18–20). Among 6157 genes on the microarray, we selected 1156 genes that are commonly methylated across >10% of AdCas and performed consensus average linkage hierarchical clustering analysis (28). In terms of DNA methylation, AdCas could be divided into three clusters, with clustering stability increasing for $k = 2$ to $k = 3$ but not for more than $k = 3$ (Figure 1A, Supplementary Figure 1, available at *Carcinogenesis* Online). Intriguingly, all four cases in cluster 1 stably fell into the same cluster regardless of *k* values (2–5), whereas 12 cases (92%) and 24 cases (96%) fell into clusters 2 and 3, respectively, indicating a high similarity of their methylation profile among each of the three-cluster member. The number of DNA methylated genes showed bimodal distribution in AdCas; DNA methylation was highly accumulated in two AdCas, both of which fell into cluster 1# (Figure 1B). Consistently, a majority of the genes were commonly methylated across more than half of the AdCas in cluster 1, whereas common methylation targets were detected in ≤50% of the AdCas in clusters 2 and 3 ($P < 0.001$, Figure 1C). In addition, the average number of methylated genes was 766.8 ± 70.4, 485.7 ± 40.6 and 319.2 ± 28.1 in clusters 1, 2 and 3 (k=3), respectively ($P < 0.001$) (Figure 1D). These observations indicated that extensively methylated AdCas exist, which appear to be characterized by correlated CpG island DNA methylation of a subset of genes in a subset of tumors, whereas AdCas with less extensive DNA methylation or with rare DNA methylation were classified into discrete subgroups (7,14–16).

Identification of CIMP markers in AdCas

MCAM analysis suggested the existence of a distinct subgroup with extensive DNA methylation in AdCas. Because CIMP status is closely associated with clinical outcome in forming a distinct subgroup in colon cancer, glioma and breast cancer (29–31), it is useful to accurately identify CIMP tumors without performing microarray analysis, which may reveal the etiology and clinical correlates of CIMP in AdCas. First, we examined whether the DNA methylation status of the classical CIMP markers (*p16*, *MINT1*, *MINT2*, *MINT31* and *MLH1*), which are effective for diagnosis of CIMP in colon cancer (32), reflected the methylation profile, especially CIMP, determined by MCAM analysis in AdCas (Figure 2A, left panel). CIMP-positive AdCas defined by the classical CIMP markers were not consistent with all the extensively methylated AdCas in cluster 1, suggesting that these markers are not always accurate for diagnosis of the extensively methylated AdCas.

To establish a new panel of a minimum number of CIMP markers without reducing the classification power, which was readily applied to a large number of tumor samples, we eliminated the genes from the target genes of methylation in MCAM analysis (Figure 2B). The initial definition of CIMP was based on concordant methylation of Type C loci (cancer-specific methylation) (7). Therefore, we first excluded markers that showed evidence of DNA methylation in normal tissues, which means Type A loci (age-related methylation) (7). Then, we selected 232 genes that were methylated in >75% of AdCas in cluster 1 but were methylated in <30% in the other clusters. Among these genes, 10 genes fulfilled the criteria of (i) concomitant array signals in all the probes for the same genes on the microarray, (ii) methylation-positive probes were located within 500 bp from transcription start sites and (iii) enable to design the stable and reproducible pyrosequencing assay using the candidate genes. Finally, we selected six candidate markers, *CCNA1*, *ACAN*, *GFRA1*, *EDARADD*, *MGC45800* and *p16* (*CDKN2A*), to determine CIMP in AdCas using a statistical model based on recursive descent partition analysis with the pyrosequencing data of 10 genes (33).

DNA methylation status of this panel of six markers was examined in 41 AdCas using pyrosequencing analysis. These six markers were frequently methylated in four (10%) AdCas of cluster 1, which showed DNA methylation in five or more of the six markers (Figure 2A, right panel). We designated this subgroup as CIMP-high (CIMP-H). In contrast, 26 (63%) AdCas were rarely methylated; none or one marker was methylated in this subgroup. The majority of AdCas (21 cases, 81%) in this subgroup fell into cluster 3, which showed the lowest frequency of DNA methylation. We defined AdCas with methylation in none or only one of the six markers as CIMP-negative (CIMP-N). The intermediate subgroup (11 cases, 27%) between CIMP-H and CIMP-N showed DNA methylation in two to four markers of the six selected CIMP markers. We designated this subgroup as CIMP-low (CIMP-L), in which 7 (64%) of 11 AdCas fell into cluster 2 and showed intermediate frequency of DNA methylation.

Validation analysis of newly identified CIMP markers

It is important to note that this initial selection of the six candidate markers did not introduce a bias for detecting CIMP only in the training set. Therefore, the newly identified panel of six markers was independently confirmed in a validation set of 87 AdCas. Among them, we found 6 (7%) CIMP-H, 30 (34%) CIMP-L and 51 (59%) CIMP-N tumors, which were of a similar frequency as observed in the training set of 41 AdCas (Supplementary Figure 2, available at *Carcinogenesis* Online). To estimate whether the classification by the six CIMP markers in the validation set was compatible with the CIMP classification in the training set, we performed the nearest four neighborhood prediction analysis (Figure 2C, see Materials and Methods). This

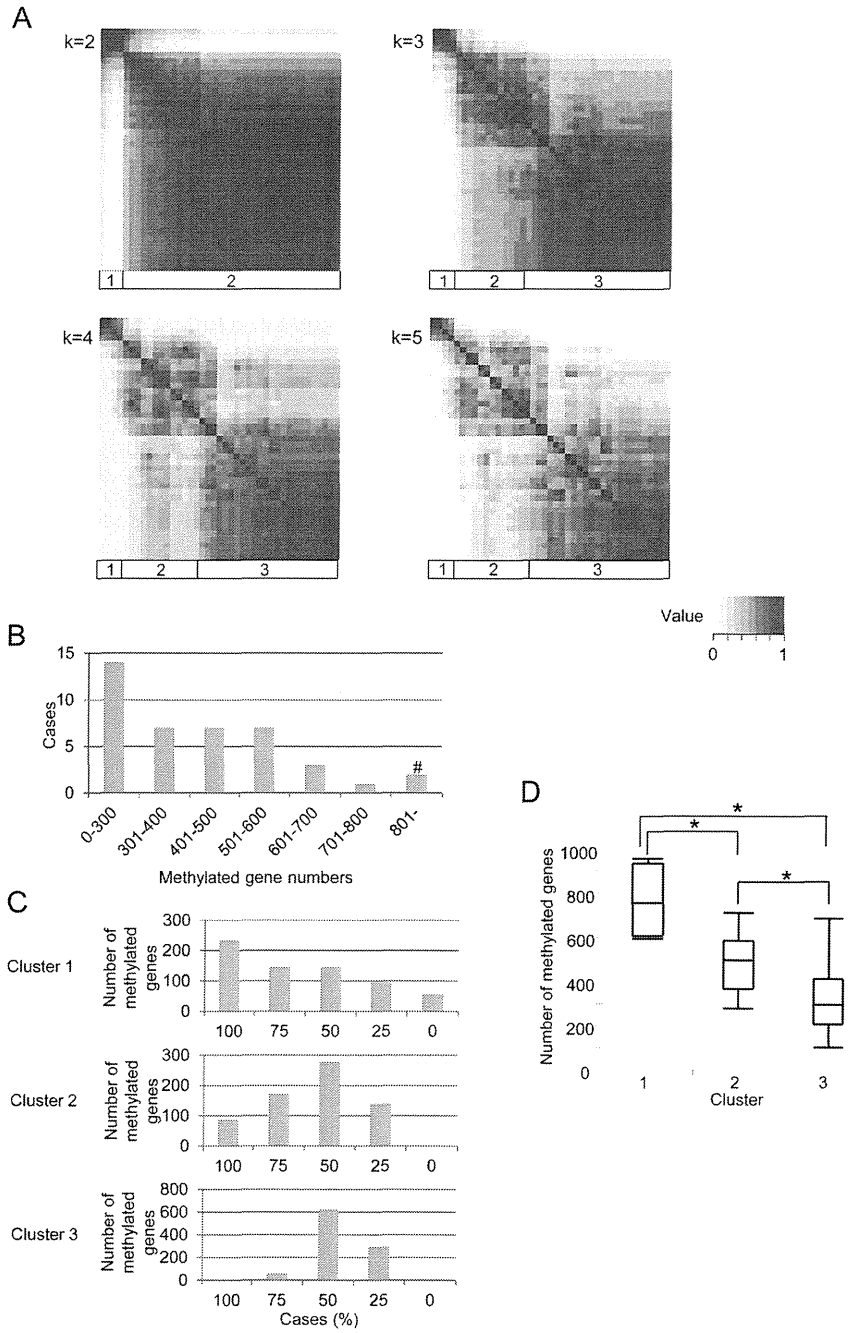

Fig. 1. DNA methylation profiling by MCAM analysis. (**A**) Consensus clustering analysis was performed with the 1156 genes from the AdCa cases for $k = 2, 3, 4$ and 5. The samples are listed in the same order on the x- and y-axes. Clusters are designated as are indicated at the bottom of each panel. Consensus index values range from 0 (highly dissimilar) to 1 (highly similar). (**B**) The distribution of number of methylated genes. X-axis indicates the number of methylated genes. Y-axis indicates cases. Two AdCas were highly methylated (#). (**C**) Distribution of number of methylated genes in each cluster. In total of 679 genes, in which methylation was observed in 20–80% of 41 AdCas, were analyzed. (**D**) Box and whisker plots of the number of methylated genes in each cluster. The mean is marked by a horizontal line inside the box whose ends denote the upper and lower quartiles. Error bars represent 5th and 95th percentile values, $^*P < 0.001$.

analysis defined 6 of 87 AdCas in the validation set as cluster 1, all of which were also categorized as CIMP-H tumors according to our criteria using the six-marker panel. Furthermore, 51 AdCas that were classified as cluster 3 with a probability >80% by the nearest neighbor classification analysis were also classified as CIMP-N tumors by our six CIMP marker panel. These results indicate that the three clusters are highly reproducible, and our panel of six markers is capable of accurately categorizing cases into these three clusters.

Identification of AdCa–CIMP in the Cancer Genome Atlas data set

Next, we examined whether the six CIMP markers could also be applicable in classifying AdCas deposited in TCGA (http://tcga-

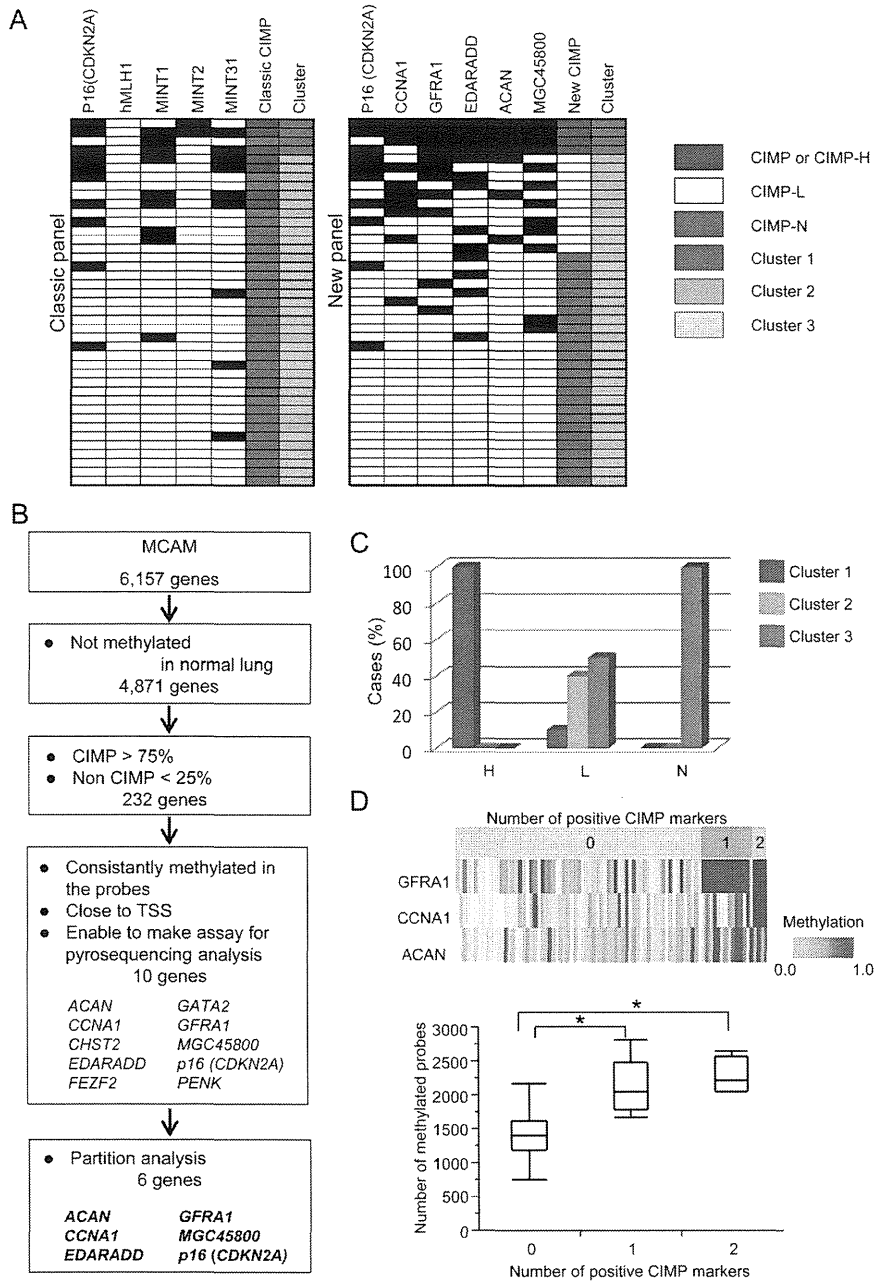

Fig. 2. DNA methylation profiling in AdCa using pyrosequencing analysis. (**A**) Comparison of classification by CIMP markers with the clusters determined by consensus clustering analysis (Figure 1A). Left: tumors with methylation in at least two of the five classical CIMP markers were determined as CIMP. Right: a panel of new CIMP markers classified CIMP-H (five or six of six markers), CIMP-L (two to four of six markers) and CIMP-N (zero or one of six markers), respectively. Black, methylation positive and white boxes, methylation negative. Clusters 1, 2 and 3 correspond to clusters 1, 2 and 3 in Figure 1A. The samples are listed in the same order on the *y*-axis in both panel. (**B**) Schema of selection for a new panel of six CIMP markers. TSS, transcription start site. (**C**) Nearest neighbor classification analysis in the validation set. Relationship between CIMP status determined by six CIMP markers, and the cluster determined by consensus cluster analysis are shown. H, CIMP-H; L, CIMP-L and N, CIMP-N. Clusters 1, 2 and 3 correspond to clusters 1, 2 and 3 in Figure 1A. (**D**) Analysis of DNA methylation status of three CIMP markers, GFRA1, CCNA1 and ACAN using the data set (3833 probes) from the Cancer Genome Atlas data set. Upper panel, heat map overview of three genes in 85 AdCas. Color corresponds to the methylation level as indicated; red is high (β value = 1.0) and yellow is low (β value = 0.0) levels of DNA methylation. Lower panel: relationship between number of methylated probes (β value > 0.4) among 3833 probes and the number of methylated genes of CIMP markers. $^{*}P < 0.001$.

data.nci.nih.gov/tcga/tcgaHome2.jsp) (30). DNA methylation data of 85 AdCas were obtained from the TCGA database, which were analyzed by the Infinium BeadChip containing 27 578 probes corresponding to 14 473 genes. Among those probes, we found that some probes corresponding to three of our new CIMP markers (*ACAN*, *CCNA1* and *GFRA1*) were located close to the regions where we conducted the pyrosequencing analysis. In contrast, no probes corresponding to the other three CIMP markers (*CDKN2A*,

MGC45800 and *EDARADD*) were located within 500 bp of transcription start sites, which was a condition of our pyrosequencing analysis. Therefore, we examined the classification power of the three CIMP markers (*ACAN*, *CCNA1* and *GFRA1*) in the 85 AdCas obtained from the TCGA. None, 4 (4.7%), 14 (16.5%) and 67 (78.8%) AdCas showed DNA methylation in three, two, one or none of the three CIMP markers, respectively (DNA methylation positive, β value > 0.4, Figure 2D, upper panel). AdCas with DNA methylation in one or two CIMP markers had more methylated probes among the 3833 most variant probes than those who had no methylation in the CIMP markers (average methylated probes: 1430.8 ± 39.5, 2116.4 ± 86.3 and 2288.8 ± 161.5, in AdCas with none, one or two methylated CIMP markers, respectively, $P < 0.001$; Figure 2D, lower panel). These data suggested that the methylation status of the three CIMP markers is also predictive for highly methylated AdCas in the TCGA data set.

Clinical significance of CIMP tumors in lung AdCa

Next, we assessed whether CIMP-positive AdCas form a distinct subgroup with characteristic clinical features. We combined two sets of AdCa cohorts (training set and validation set) for the analysis of CIMP signatures, with a total of 128 cases. We did not access any clinical information before CIMP classification of both sets of AdCas to avoid any bias in the analysis of the clinical significance of CIMP tumors. Of the 128 pooled AdCas, 10 (7.8%) were classified as CIMP-H, 40 (31.3%) as CIMP-L and 78 (60.9%) as CIMP-N (Figure 3A). CIMP-H tumors were more prevalent in males ($P = 0.0047$) and associated with frequent exposure to smoking (pack year > 40, $P = 0.0036$). Intriguingly, we found a tight association between CIMP and *EGFR* status ($P = 0.0089$; Table I). None of the 10 CIMP-H AdCas contained any *EGFR* mutations, whereas 36/78 (46.2%) CIMP-N and 12/40 (30.0%) CIMP-L AdCas had *EGFR* mutations. In contrast, no such tendency was observed between CIMP status and *KRAS*, *TP53* and *BRAF* mutations.

To investigate whether CIMP status had any impact on overall survival, we performed Kaplan–Meier survival analysis and found that CIMP-H was a significantly negative prognostic factor ($P = 0.0115$, log-rank test; Figure 3B). Since *EGFR* mutations have been indicated as a potential positive prognostic factor for survival in advanced non-small cell lung cancer patients treated with chemotherapy with or without TKI (34), we analyzed overall survival according to the *EGFR* mutation status. Among the AdCas harboring wild-type *EGFR*, CIMP-H tumors still correlated with poor survival ($P = 0.0312$, log-rank test; Figure 3C). In addition to a worse prognosis in patients with AdCas who were smokers ($P = 0.0373$, log-rank test; Figure 3D), we found that CIMP-H was an independent prognostic factor among male smokers (hazard ratio 1.7617, 95% confidence interval 1.0030–2.9550, $P = 0.0489$; Figure 3E). Taken together, these findings indicated that CIMP-H tumors have unique clinical features that distinguish them from the other AdCas.

Clinical implication of epigenetic therapy for lung AdCa

To evaluate the relationship between CIMP status and effects of the DNA methylation inhibitor, 5-Aza-dC, as an antitumor agent, we first analyzed DNA methylation status of the six CIMP markers in 14 AdCa cell lines, including one CIMP-H (H358), seven CIMP-L (H23, H1, PC9, H2009, H3255, H1975 and H1650) and six CIMP-N cell lines (H920, A549, HCC827, ML13, H1573 and HCC4011) (Supplementary Table 4, available at *Carcinogenesis* Online). CIMP-H cells (H358) harbor wild-type *EGFR*, whereas the CIMP-L and CIMP-N cells harbor either wild-type (H23, H1, H2009, H1975, H920, A549, HCC827, ML13 and H1573) or mutated (PC9, H3255, H1650 and HCC4011) *EGFR*. Regardless of the CIMP status, cells with wild-type *EGFR* showed resistance to the TKI, AG1478 (Figure 4A). Intriguingly, antitumor activity of 5-Aza-dC appeared to be associated with CIMP status. Each cell line showed different IC50, which were significantly lower in the CIMP-positive cells (average, CIMP-H and CIMP-L) than in the CIMP-N cells ($P = 0.02$, average IC50 was 68, 229 and 982 nM, respectively, Figure 4B). To determine a more accurate relationship between DNA demethylation and antitumor activity, we used level of *LINE-1* demethylation, which represents the global level of methylation, as a surrogate marker of 5-Aza-dC treatment. We examined the power of growth inhibition at a concentration of ~20% of *LINE-1* demethylation. Cell growth of CIMP-H and CIMP-L cells was significantly inhibited at each concentration of 5-Aza-dC, in contrast to CIMP-N cells, the majority of which did not respond to the treatment (Figure 4B). These data suggest that in addition to CIMP-H AdCas, tumorigenesis of CIMP-L AdCas may also depend on DNA methylation silencing pathway to some extent.

Discussion

In the current study, we performed a comprehensive genome-wide DNA methylation analysis and identified a distinct molecular subgroup (CIMP-H) in human AdCas. This subgroup showed a remarkably high rate of DNA methylation in correlated cancer-specific CpG island hypermethylation of a subset of genes, indicating the existence of CIMP in AdCas (7).

Previously, studies suggested the existence of CIMP in lung cancer. The first study defined a CIMP-positive case as having a tumor with aberrant methylation in either *CDH13* or *CRBP1* and found that CIMP-positive cases showed poorer prognosis than the CIMP-N ones (9). Although a consistent clinical feature, poor prognosis of CIMP-positive cases, was observed between our study and the previous ones, frequencies of CIMP and the other clinicopathological features associated with CIMP were varied, probably due to the different panels of CIMP marker examined (9,11–13). Thus, it is still unclear which DNA methylation markers can define the most extensively methylated subgroups (CIMP) due to the lack of accompanied genome-wide analysis in the previous AdCa studies. If CIMP affects only a subset of CpG islands in a subgroup of AdCas, collection of data for a large numbers of markers from numerous tumor samples is required to identify CIMP in AdCas. Indeed, we found in the current study that CIMP-positive tumors diagnosed by the original CIMP markers defined in the colon cancer study (7) were not consistent with the extensively methylated AdCas, suggesting that these markers are not always applicable for diagnosis of CIMP tumors other than colon cancers. Thus, the existence of CIMP in AdCas from the global point of view has remained elusive before the current study. Our genome-wide MCAM analysis successfully identified six practical and representative markers for the prediction of CIMP in AdCas.

Integrated analysis of the DNA methylation status of the six CIMP markers with several cancer-associated gene mutations, including *EGFR*, *TP53*, *KRAS* and *BRAF*, revealed that CIMP-H tumors in both the training and the validation sets did not harbor any *EGFR* mutations, suggesting that the two events are mutually exclusive, whereas mutations in the other three genes did not show such strong associations with CIMP status. Thus, our six novel markers enabled us to decipher the negative association between CIMP and *EGFR* mutations, which had been only suggested by previous studies (35). Indeed, CIMP-H tumors are significantly associated with males, frequent exposure to smoking and high relapse rate of disease, which clearly differ from the typical features of *EGFR*-mutant AdCas, such as association with females, non-habit forming smoking and better prognosis. Interestingly, colorectal cancers also show strong association between CIMP status and smoking (36,37). Thus, smoking may be one of the potential causes of CIMP. These data suggested that a particular set of genes are methylated in CIMP-H AdCas, and their target genes are involved in activation of an alternative pathway, in which tumorigenesis may be minimally dependent on *EGFR* mutation.

The association of better clinical outcome with CIMP-positive tumors has been reported in breast cancer, colon cancer and glioma. Fang *et al.* (31) showed that there was significant overlap of CIMP targets in those different types of cancers. Among the 33 overlapped CIMP targets between the cancers, we found that the DNA methylation status of 19 genes was available from our MCAM analysis. Using

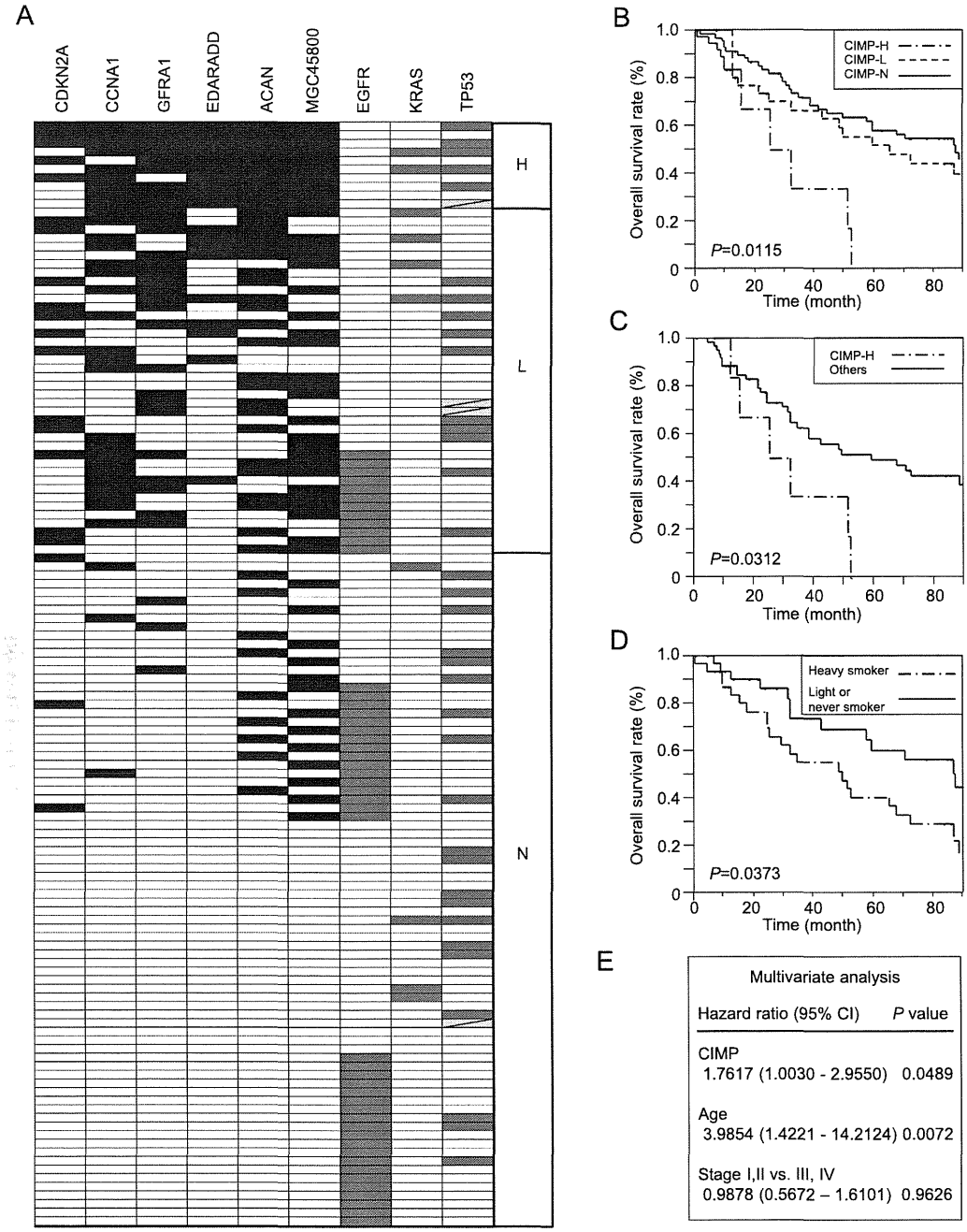

Fig. 3. CIMP status associated with prognosis of AdCas. (**A**) Total of 128 AdCas were classified into three subclasses by the six newly identified CIMP markers. Black boxes, methylation positive; gray boxes, mutation positive; white boxes, methylation negative or mutation negative and light gray boxes with oblique lines, data were not available for *TP53* status. H, CIMP-H; L, CIMP-L and N, CIMP-N. (**B**) Kaplan–Meier analysis for overall survival of 128 AdCa patients by CIMP status. *P* value was calculated by log-rank analysis. (**C**) Kaplan–Meier analysis for overall survival of 80 AdCas cases harboring wild-type *EGFR* by CIMP status. (**D**) Kaplan–Meier analysis for overall survival by smoking status. (**E**) Multivariate analysis showed that CIMP-H was an independent prognostic factor among male smokers (n = 37).

the methylation status of these 19 genes, we found that AdCas in our training set were divided into three clusters; the three most extensively methylated AdCas were consistent with the CIMP-H AdCas, suggesting that a panel of 19 genes may also be a potent predictor for CIMP-H in AdCas (Supplementary Figure 3, available at *Carcinogenesis* Online). However, given the worse prognosis of patients with CIMP-H AdCas, the impact of CIMP to survival in lung cancer might be different from the CIMP in colon cancer, glioma and breast cancer. Indeed, a study in myelodysplastic syndromes also showed that the presence of CIMP was significantly associated with poor prognosis and risk of leukemia transformation (38). The contrasting impacts of CIMP to clinical outcome might be due to the distinct DNA methylation profiles specific to each tumor type; CIMP confers poor prognosis in lung AdCas and myelodysplastic syndromes via inactivation

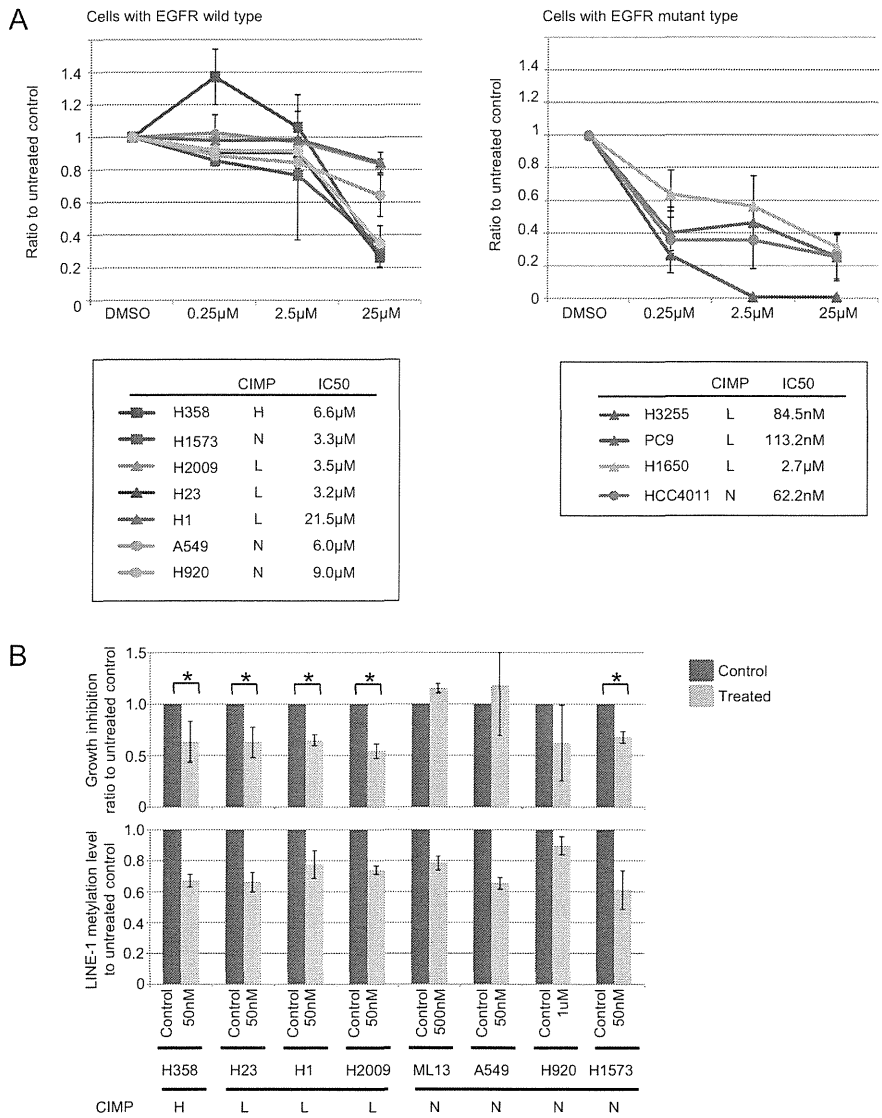

Fig. 4. Epigenetic treatment in AdCa cell lines. (**A**) Growth rate of AdCa cell lines with each *EGFR* status as measured by 3-(4,5-dimethylthiazole-2-yl)-2,5-bdiphenyl tetrazolium bromide assay after 72 h of treatment of TKI (AG1478) in different doses. CIMP status of each cell line is indicated by H, L and N. (**B**) Growth inhibition of AdCas after 5-Aza-dC treatment. Growth inhibition was examined (upper panel) at the concentration where 20% of LINE-1 demethylation had occurred (lower panel). $^{*}P < 0.05$.

of genes critical for tumor progression and for response to chemotherapy.

We found another epigenomic subgroup (CIMP-L) of AdCas within the major subclasses classified by DNA methylation status. This subtype showed moderate accumulation of DNA methylation. Indeed, our cell line study showed that CIMP-L cells were sensitive to 5-Aza-dC treatment. These data suggest that tumorigenesis pathway of CIMP-L AdCas might also be affected by DNA methylation to a certain extent. However, we could not find any specific features of this subtype. This might be due to the lack of suitable markers to further classify CIMP-L, resulting in a mixture of subpopulations as was found in the colon cancer study (39,40). Sensitive and specific markers for CIMP-L in AdCas are needed to further characterize CIMP-L. Additional studies will be required to address this problem.

CIMP-positive lung AdCa cell lines appeared to be more sensitive to 5-Aza-dC treatment, in which demethylation effectively occurred even at low doses of 5-Aza-dC, regardless of *EGFR* mutation status. Epigenetic drugs targeting DNA methylation, such as 5-Aza-dC and 5-azacytidine, have shown clinical effectiveness in cancer treatment, especially for hematological malignancies (41,42). For the treatment of thoracic malignancies, studies showed that a certain population of patients with AdCas clinically benefit from 5-Aza-dC treatment (43,44). One of the important issues of research is the identification of biomarkers predictive of response to DNA methylation inhibitors (45). Our cell line analysis showed that CIMP status appeared to be associated with response to 5-Aza-dC, suggesting that epigenetic therapy might be a useful approach, especially for those individuals who have been diagnosed with CIMP. If this possibility was validated, our findings would be significant for the use of DNA methylation inhibitors in lung tumors.

In conclusion, we demonstrated here that six newly identified CIMP markers may be useful in the accurate and practical epigenomic

classifications of lung cancer. Our findings may enable the development of new molecular diagnostics tools for personalized medicine for lung cancers and confer a new paradigm for cancer treatment.

Supplementary material

Supplementary Figures 1–3 and Tables 1–4 can be found at http://carcin.oxfordjournals.org/.

Funding

This work is supported by grants-in-aid for Cancer Research from the Ministry of Health. Labor and Welfare (to Y.K.) and a grant from the Japan Society for the Promotion of Science (to Y.K.).

Conflict of Interest Statement: None declared.

References

1. Jemal,A. *et al.* (2010) Cancer statistics, 2010. *CA Cancer J. Clin.*, **60**, 277–300.
2. Mitsudomi,T. *et al.* (2010) Gefitinib versus cisplatin plus docetaxel in patients with non-small-cell lung cancer harbouring mutations of the epidermal growth factor receptor (WJTOG3405): an open label, randomised phase 3 trial. *Lancet Oncol.*, **11**, 121–128.
3. Choi,Y.L. *et al.* (2010) EML4-ALK mutations in lung cancer that confer resistance to ALK inhibitors. *N. Engl. J. Med.*, **363**, 1734–1739.
4. Belinsky,S.A. (2004) Gene-promoter hypermethylation as a biomarker in lung cancer. *Nat. Rev. Cancer*, **4**, 707–717.
5. Jones,P.A. *et al.* (2002) The fundamental role of epigenetic events in cancer. *Nat. Rev. Genet.*, **3**, 415–428.
6. Jones,P.A. *et al.* (2007) The epigenomics of cancer. *Cell*, **128**, 683–692.
7. Toyota,M. *et al.* (1999) CpG island methylator phenotype in colorectal cancer. *Proc. Natl Acad. Sci. USA*, **96**. 8681–8686.
8. Grady,W.M. (2007) CIMP and colon cancer gets more complicated. *Gut*, **56**, 1498–1500.
9. Suzuki,M. *et al.* (2006) Exclusive mutation in epidermal growth factor receptor gene, HER-2, and KRAS, and synchronous methylation of non-small cell lung cancer. *Cancer*, **106**, 2200–2207.
10. Marsit,C.J. *et al.* (2006) Examination of a CpG island methylator phenotype and implications of methylation profiles in solid tumors. *Cancer Res.*, **66**, 10621–10629.
11. Liu,Z. *et al.* (2008) CpG island methylator phenotype involving tumor suppressor genes located on chromosome 3p in non-small cell lung cancer. *Lung Cancer*, **62**, 15–22.
12. Suzuki,M. *et al.* (2010) Molecular characterization of chronic obstructive pulmonary disease-related non-small cell lung cancer through aberrant methylation and alterations of EGFR signaling. *Ann. Surg. Oncol.*, **17**, 878–888.
13. Zhang,Y. *et al.* (2011) Methylation of multiple genes as a candidate biomarker in non-small cell lung cancer. *Cancer Lett.*, **303**, 21–28.
14. Weisenberger,D.J. *et al.* (2006) CpG island methylator phenotype underlies sporadic microsatellite instability and is tightly associated with BRAF mutation in colorectal cancer. *Nat. Genet.*, **38**, 787–793.
15. Ogino,S. *et al.* (2006) CpG island methylator phenotype-low (CIMP-low) in colorectal cancer: possible associations with male sex and KRAS mutations. *J. Mol. Diagn.*, **8**, 582–588.
16. Shen,L. *et al.* (2007) Integrated genetic and epigenetic analysis identifies three different subclasses of colon cancer. *Proc. Natl Acad. Sci. USA*, **104**, 18654–18659.
17. Gao,W. *et al.* (2008) Variable DNA methylation patterns associated with progression of disease in hepatocellular carcinomas. *Carcinogenesis*, **29**, 1901–1910.
18. Goto,Y. *et al.* (2009) Epigenetic profiles distinguish malignant pleural mesothelioma from lung adenocarcinoma. *Cancer Res.*, **69**, 9073–9082.
19. An,B. *et al.* (2010) A characteristic methylation profile in CpG island methylator phenotype-negative distal colorectal cancers. *Int. J. Cancer*, **127**, 2095–2105.
20. Okamoto,Y. *et al.* (2012) Aberrant DNA methylation associated with aggressiveness of gastrointestinal stromal tumour. *Gut*, **61**, 392–401.
21. Yang,A.S. *et al.* (2004) A simple method for estimating global DNA methylation using bisulfite PCR of repetitive DNA elements. *Nucleic Acids Res.*, **32**, e38.
22. Kondo,Y. *et al.* (2007) Alterations of DNA methylation and histone modifications contribute to gene silencing in hepatocellular carcinomas. *Hepatol Res.*, **37**, 974–983.
23. Eisen,M.B. *et al.* (1998) Cluster analysis and display of genome-wide expression patterns. *Proc. Natl Acad. Sci. USA*, **95**, 14863–14868.
24. Cover,T. *et al.* (1967) Nearest neighbor pattern classification. *IEEE Trans. Inform. Theory*, **13**, 21–27.
25. Yokoyama,T. *et al.* (2006) EGFR point mutation in non-small cell lung cancer is occasionally accompanied by a second mutation or amplification. *Cancer Sci.*, **97**, 753–759.
26. Ogino,S. *et al.* (2005) Sensitive sequencing method for KRAS mutation detection by pyrosequencing. *J. Mol. Diagn.*, **7**, 413–421.
27. Spittle,C. *et al.* (2007) Application of a BRAF pyrosequencing assay for mutation detection and copy number analysis in malignant melanoma. *J. Mol. Diagn.*, **9**, 464–471.
28. Monti,S. *et al.* (2003) Consensus clustering: a resampling-based method for class discovery and visualization of gene expression microarray data. *Mach. Learn.*, **52**, 91–118.
29. Toyota,M. *et al.* (2000) Distinct genetic profiles in colorectal tumors with or without the CpG island methylator phenotype. *Proc. Natl Acad. Sci. USA*, **97**, 710–715.
30. Noushmehr,H. *et al.* (2010) Identification of a CpG island methylator phenotype that defines a distinct subgroup of glioma. *Cancer Cell*, **17**, 510–522.
31. Fang,F. *et al.* (2011) Breast cancer methylomes establish an epigenomic foundation for metastasis. *Sci. Transl. Med.*, **3**, 75ra25.
32. Issa,J.P. (2004) CpG island methylator phenotype in cancer. *Nat. Rev. Cancer*, **4**, 988–993.
33. Lu,K.H. *et al.* (2004) Selection of potential markers for epithelial ovarian cancer with gene expression arrays and recursive descent partition analysis. *Clin. Cancer Res.*, **10**, 3291–3300.
34. Eberhard,D.A. *et al.* (2005) Mutations in the epidermal growth factor receptor and in KRAS are predictive and prognostic indicators in patients with non-small-cell lung cancer treated with chemotherapy alone and in combination with erlotinib. *J. Clin. Oncol.*, **23**, 5900–5909.
35. Toyooka,S. *et al.* (2006) Mutational and epigenetic evidence for independent pathways for lung adenocarcinomas arising in smokers and never smokers. *Cancer Res.*, **66**, 1371–1375.
36. Samowitz,W.S. *et al.* (2006) Association of smoking, CpG island methylator phenotype, and V600E BRAF mutations in colon cancer. *J. Natl Cancer Inst.*, **98**. 1731–1738.
37. Limsui,D. *et al.* (2010) Cigarette smoking and colorectal cancer risk by molecularly defined subtypes. *J. Natl Cancer Inst.*, **102**, 1012–1022.
38. Shen,L. *et al.* (2010) DNA methylation predicts survival and response to therapy in patients with myelodysplastic syndromes. *J. Clin. Oncol.*, **28**, 605–613.
39. Ogino,S. *et al.* (2008) Molecular classification and correlates in colorectal cancer. *J. Mol. Diagn.*, **10**, 13–27.
40. Yagi,K. *et al.* (2010) Three DNA methylation epigenotypes in human colorectal cancer. *Clin. Cancer Res.*, **16**, 21–33.
41. Silverman,L.R. *et al.* (2002) Randomized controlled trial of azacitidine in patients with the myelodysplastic syndrome: a study of the cancer and leukemia group B. *J. Clin. Oncol.*, **20**, 2429–2440.
42. Kantarjian,H. *et al.* (2006) Decitabine improves patient outcomes in myelodysplastic syndromes: results of a phase III randomized study. *Cancer*, **106**, 1794–1803.
43. Schrump,D.S. *et al.* (2006) Phase I study of decitabine-mediated gene expression in patients with cancers involving the lungs, esophagus, or pleura. *Clin. Cancer Res.*, **12**, 5777–5785.
44. Momparler,R.L. *et al.* (2001) Potential of 5-aza-2'-deoxycytidine (Decitabine) a potent inhibitor of DNA methylation for therapy of advanced non-small cell lung cancer. *Lung Cancer*, **34** (suppl. 4), S111–S115.
45. Garcia-Manero,G. (2010) Prognosis of myelodysplastic syndromes. *Hematology Am. Soc. Hematol. Educ. Program*, **2010**, 330–337.

Received November 20, 2011; revised April 9, 2012; accepted April 18, 2012